Malvern Panalytical

Resolution in Reciprocal Space

Understanding the Experiment

Outline

- Understanding the experiment in real and reciprocal space
- Resolution in reciprocal space
- Interpreting the data in real and reciprocal space
- Simulation of rocking curves using dynamical diffraction theory
- Calculations of relaxation and composition from peak positions
- Lateral size effects observed in maps
- General observations in maps to reveal microstructure

Which Scan Axes Are Used?

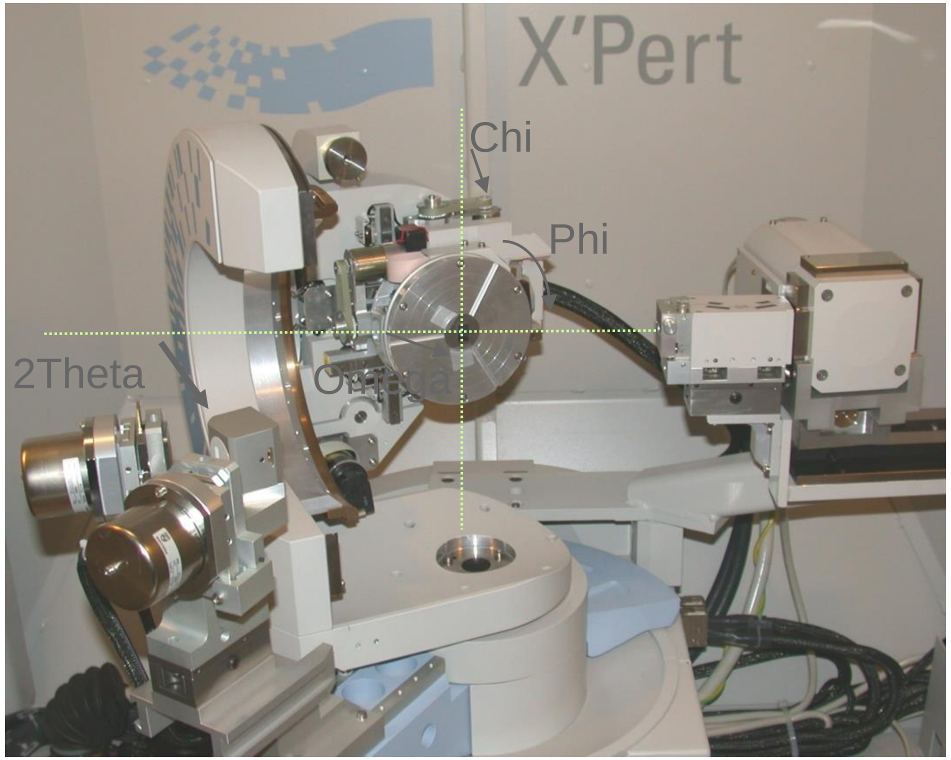

High resolution:

- Omega scans, open detector (HR)
- Omega/2Theta scans, triple axis (TA)
- Omega/2Theta x Omega maps (TA)

Low resolution:

- 2Theta/Omega scans
- 2Theta/Omega x Omega maps
- Phi and Chi are used primarily for alignment

Scans Supported by Analysis in X'Pert Epitaxy [1]

Reciprocal Space Maps ("Maps")

- Collected as a series of Omega/2Theta scans around a Bragg peak. Each scan is at a different Omega offset value.
- Used with triple bounce analyzer (TA optics)*.
- Suitable for slightly defective single crystal semiconductors.
- Can be analyzed in a map through calculations related to peak positions and peak widths.

* Recommended. Variations are possible.

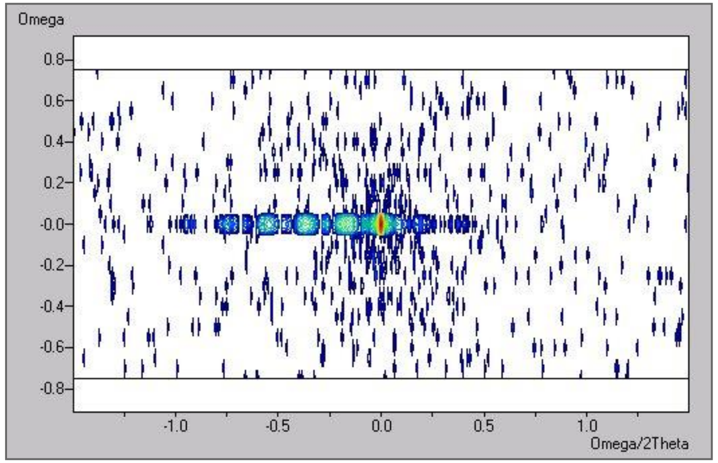

Scans Supported by Analysis in X’Pert Epitaxy [2]

Rocking Curves

- Collected as a single Omega scan around a Bragg peak.
- Used with an open detector (HR optics)**.
- Suitable for highly perfect single crystal semiconductors.
- Can be analyzed through calculations related to peak separations.
- Can be simulated by dynamical diffraction theory.

** Recommended. Variations are possible.

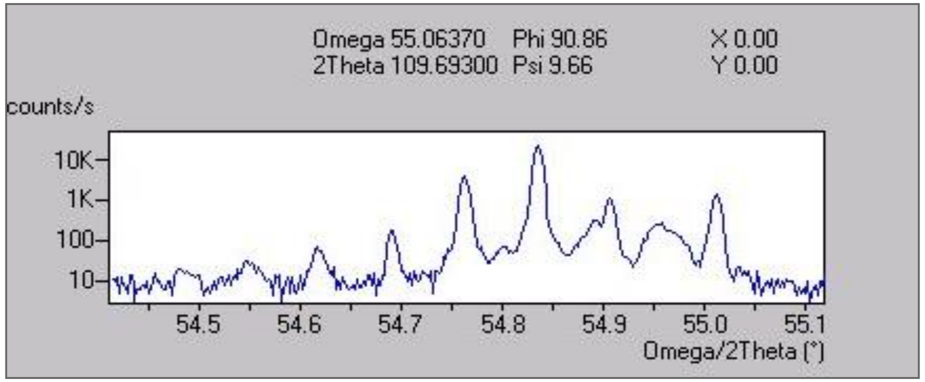

Materials Measured Using Maps

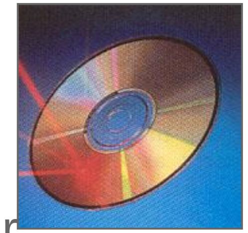

Maps

- Any materials
  - Although not traditionally used for powders they can be used for example to show crystallization or to reveal preferred orientation.
  - Polycrystalline thin films and textured thin films tend to show weaker and larger features and may require lower resolution optics.
  - Single crystals and semiconductors (with or without epitaxial layers) show stronger and finer features and require high resolution optics.

Materials Measured Using Rocking Curves

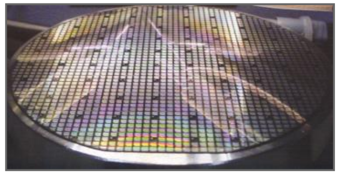

Rocking Curves

- Flat single crystals e.g. highly perfect single crystal semiconductor wafers.
- Strained epitaxial layers and device-type structures.
- Epitaxial layers with some misfit dislocations (‘relaxed epitaxial layers‘).

Understanding the Experiment in Real and Reciprocal Space

Real Space Visualization of the Experiment

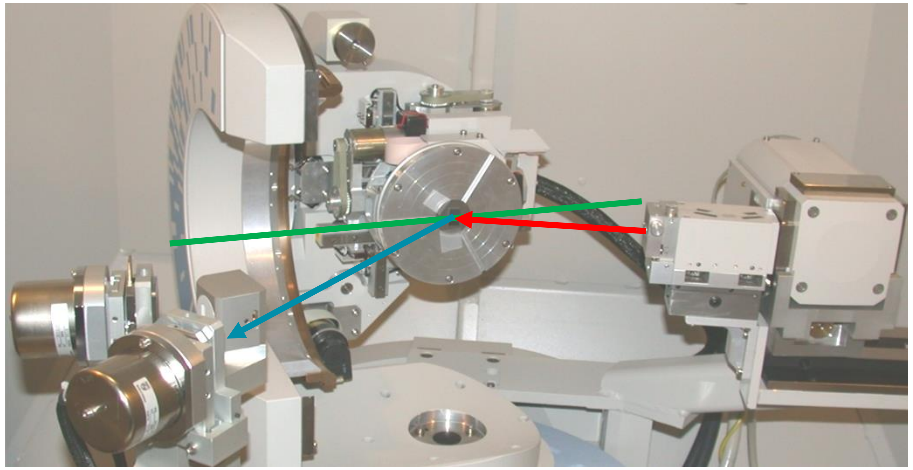

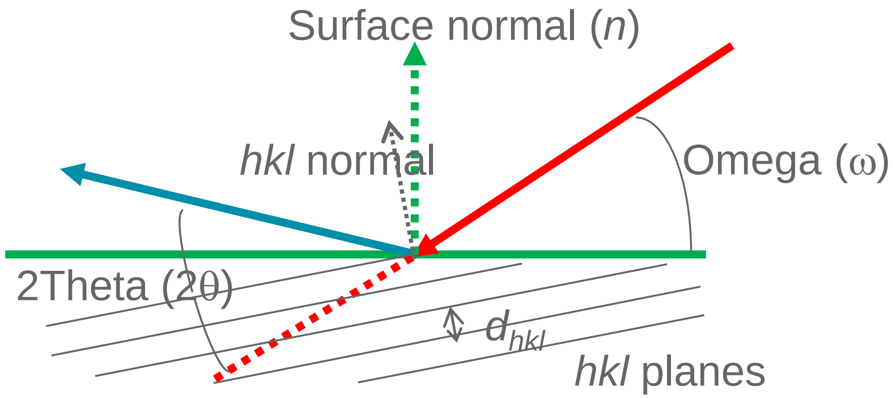

Real space beam directions

The plane containing the incident and detected beam is called the ***Diffraction Plane***

The Experiment in Diffraction Space Vectors

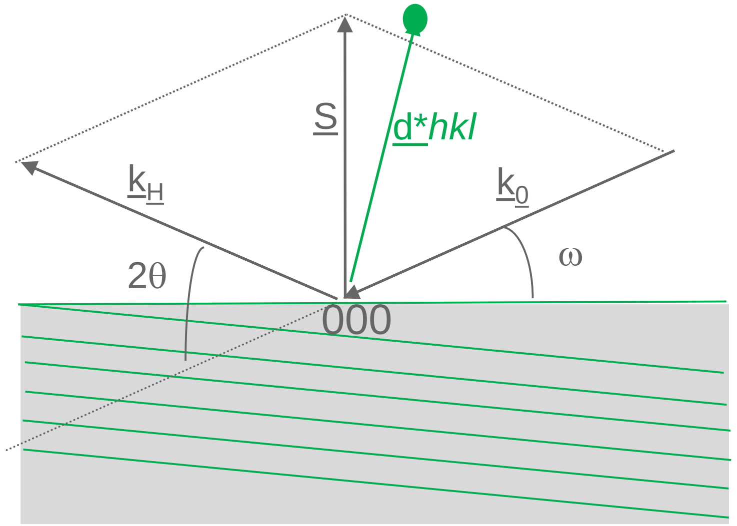

By rotating $\underline{k_H}$ and $\underline{k_0}$, the diffraction vector $\underline{S}$ can be made to scan through reciprocal space.

When $\underline{S} = \underline{d^*hkl}$, then Bragg diffraction occurs

$\underline{d^*hkl}$	Reciprocal lattice vector $\underline{d^*hkl}$ Length 1/d Direction normal to *hkl* planes
$\underline{k_0}$	Incident beam vector, $\underline{k_0}$ Length n/λ (user-defined) Direction ω defined relative to sample surface
$\underline{k_H}$	Scattered beam vector $\underline{k_H}$ Length n/λ (user-defined) Direction 2θ defined relative to ω = 0
$\underline{S}$	Diffraction vector $\underline{S} = \underline{k_H} - \underline{k_0}$

Visualization of an Omega/2Theta* Scan

Symmetric Omega/2Theta* scan
(no offset)

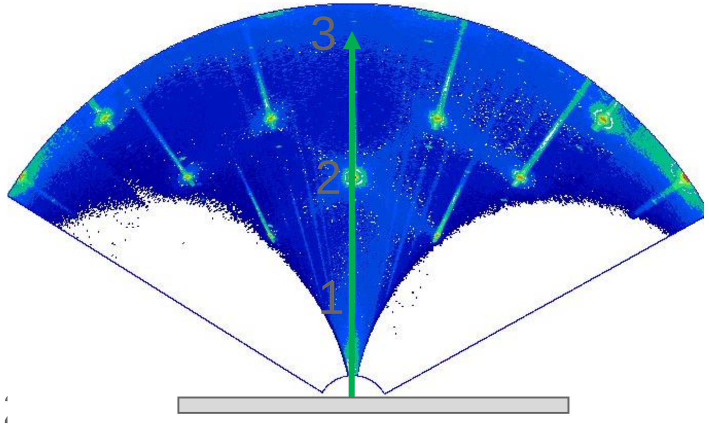

* or

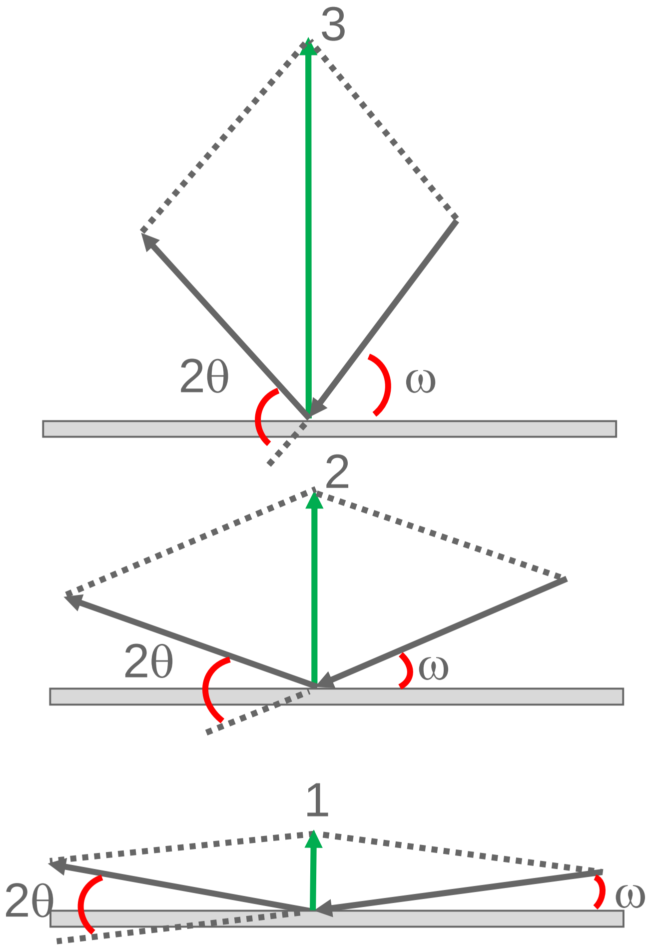

Visualization of an Omega/2Theta* Scan with +Offset

Omega > 2Theta/2

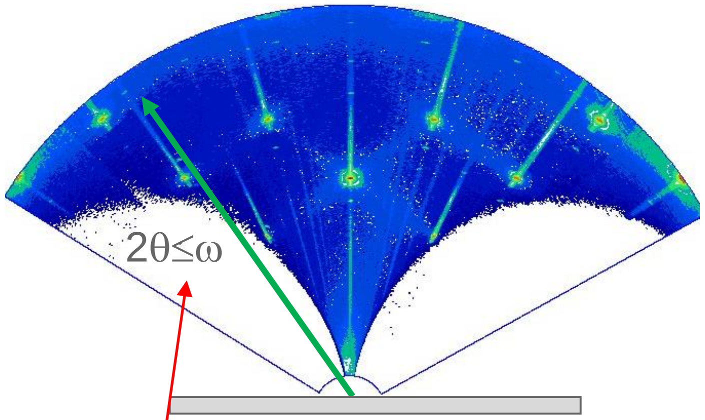

No exit for diffracted beam

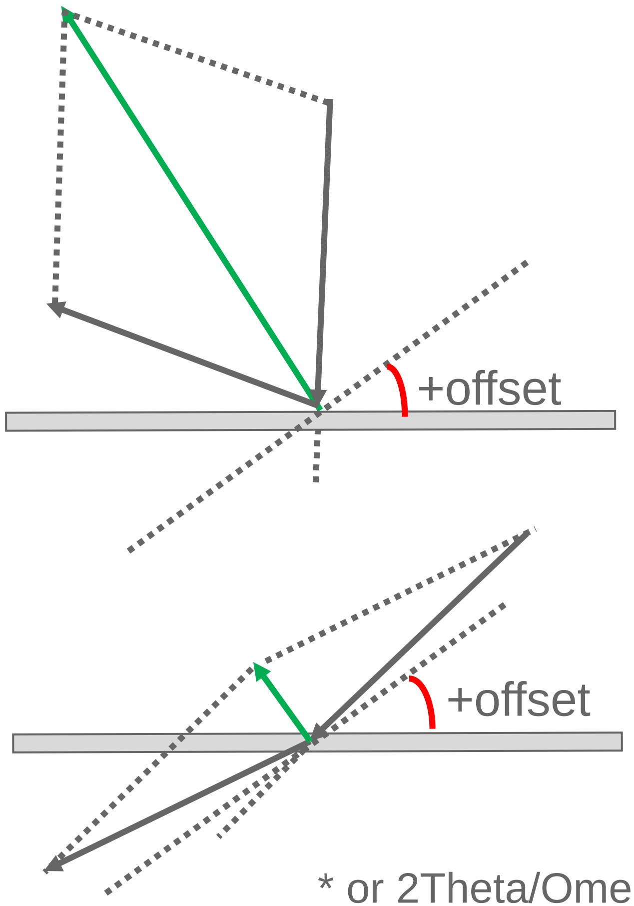

* or 2Theta/Omega

Visualization of an Omega/2Theta* Scan with -Offset

Omega < 2Theta/2

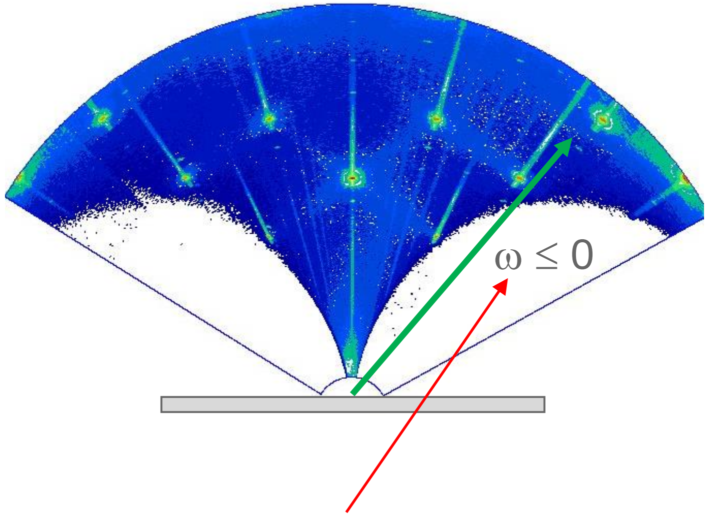

No

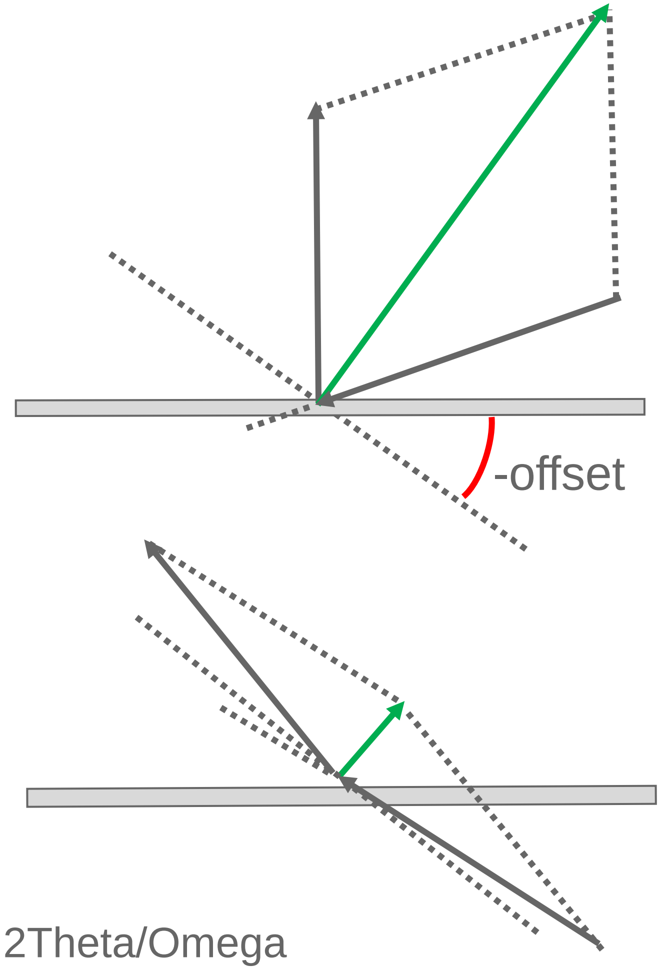

* or 2Theta/Omega

Map: Collection of Omega/2Theta Scans

Large area map displayed using X'Pert Epitaxy

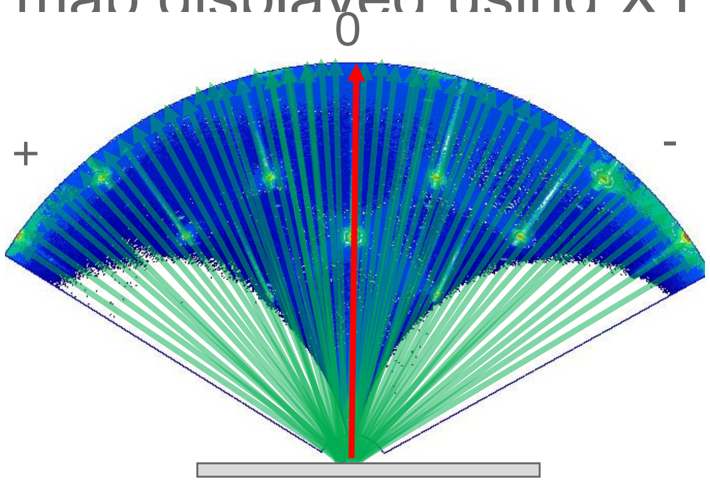

Reciprocal space view

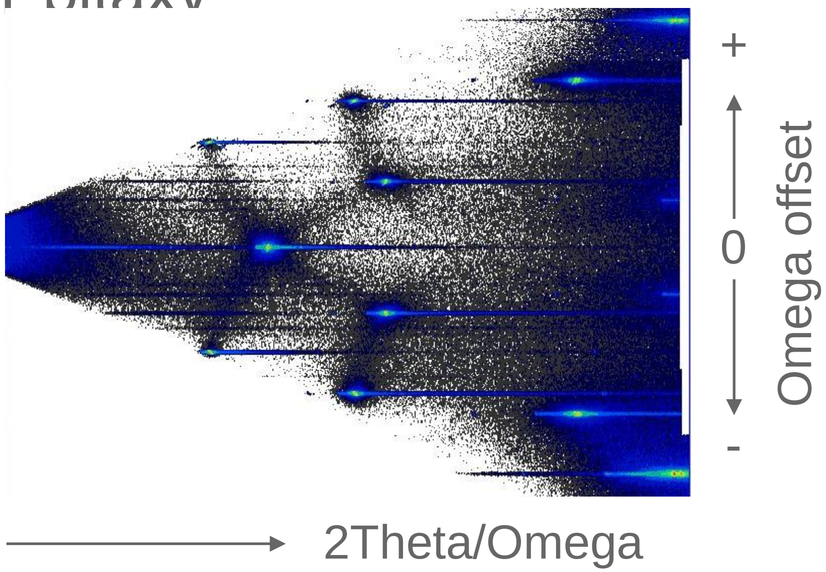

Data collection view

Small Area Collected at High Resolution

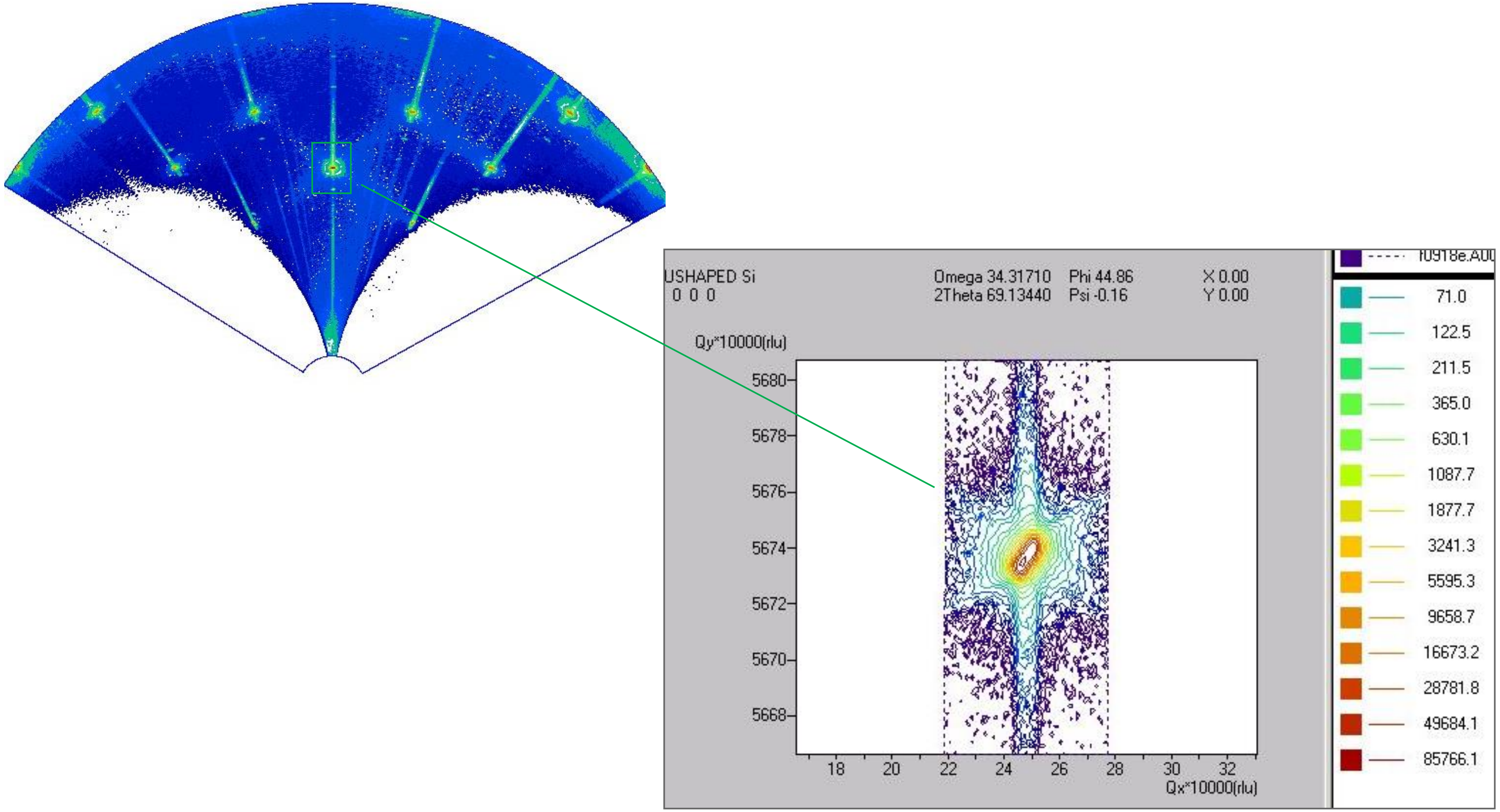

Reciprocal Space Coordinates

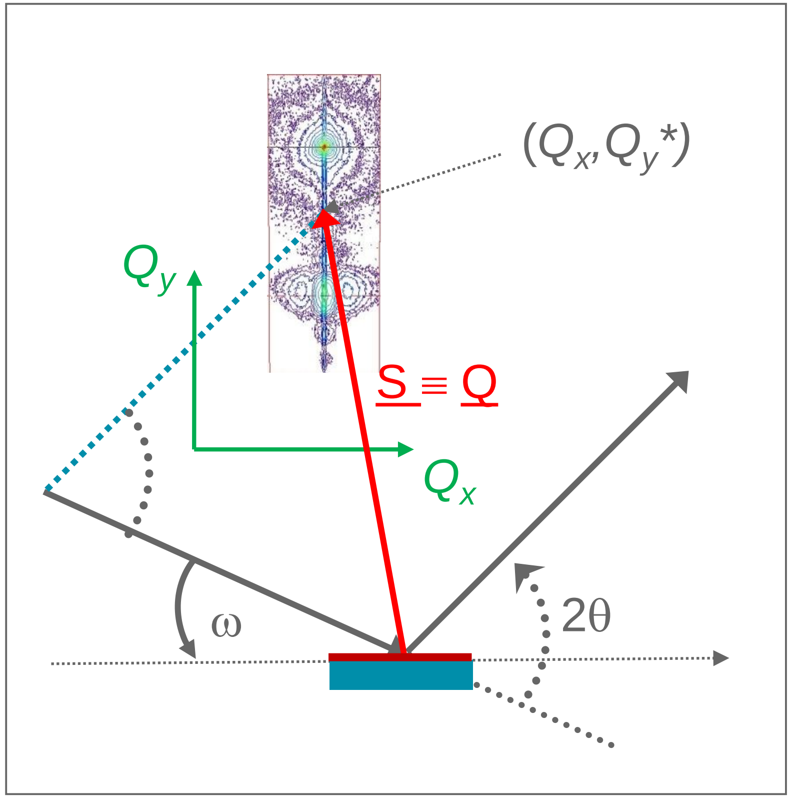

A reciprocal space map is displayed with collected intensity I (cps), denoted by color contours. The sample (ω) and detector (2θ) angles are converted to provide the coordinates of the diffraction vector <u>S</u> (or <u>Q</u>) in reciprocal lattice units (Q_x,Q_y^*).

where: $Q_x = R\,[\cos\omega - \cos(2\theta - \omega)]$
and $Q_y^* = R\,[\sin\omega + \sin(2\theta - \omega)]$

R (length of incident and scattered beam vector) can take various values depending upon the most convenient form for the user, e.g 2π/λ, 1/λ (recommended), 1, ½.

In X'Pert Epitaxy. input your own value for R in *"customise/defaults/Qscan & area scan rlu value".*

* Sometimes Q_z is used rather than Q_y to denote the direction perpendicular to the sample surface.

Ewald Sphere: Reciprocal Space and Bragg's Law

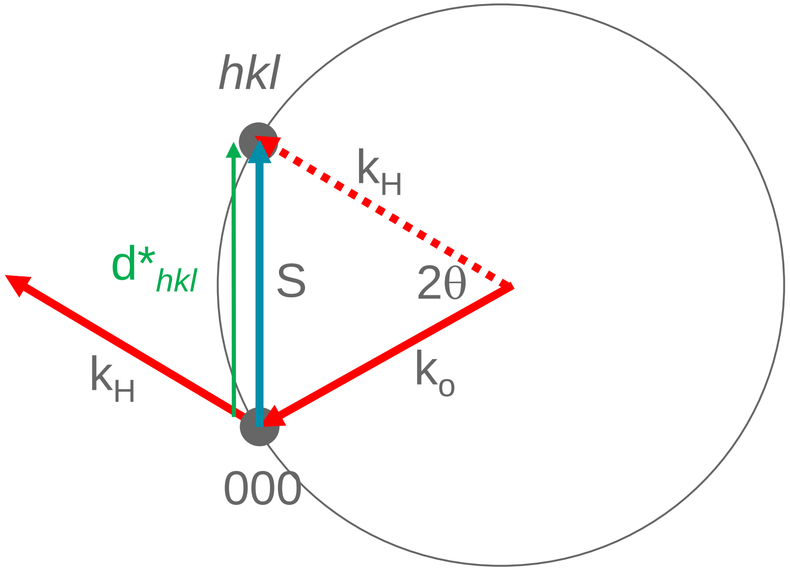

k_o	incident beam vector
k_H	diffracted beam vector
S	scattering vector
d^*_{hkl}	reciprocal lattice vector

- Vector algebra

  $k_o - k_H = S$

  At maximum intensity:

  $S = d^*_{hkl}$

- Trigonometry

  $|k| = 1/\lambda$

  $|d^*_{hkl}| = 1/d$

  $\sin\theta = \lambda/2d$

  $\lambda = 2d \sin\theta$

Reciprocal Lattice Vector

- Reciprocal lattice points are derived from the crystallographic planes in the sample and the orientation of the sample in the experiment.
- Create reciprocal lattice (RL), where each point represents a set of planes *(hkl).*
- The points are generated from the origin (000) where the vector, $d_{*(hkl)}$, from the origin to the RLP has the direction of the plane normal and length given by the reciprocal of the plane spacing.

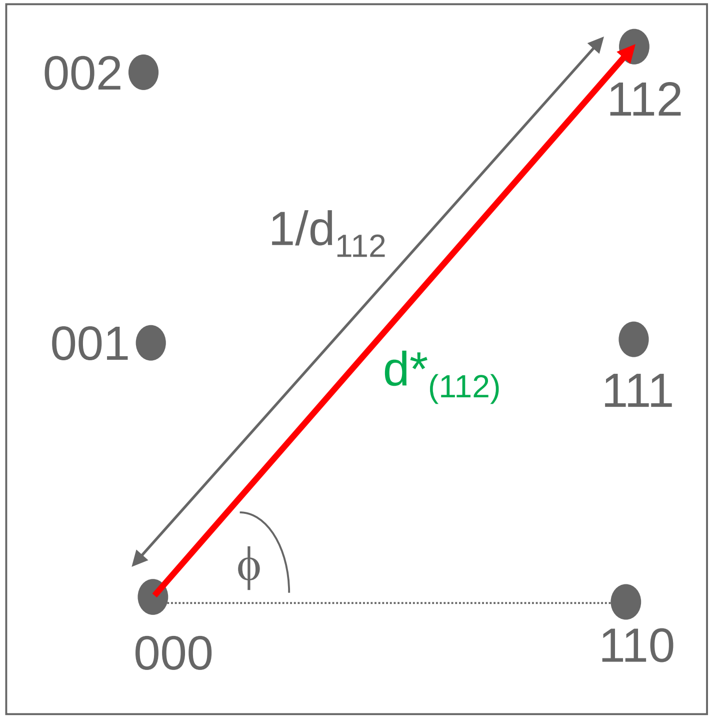

Reciprocal Space Structure of Single Crystals

At peak intensity, S= r* (magnitude 1/d)

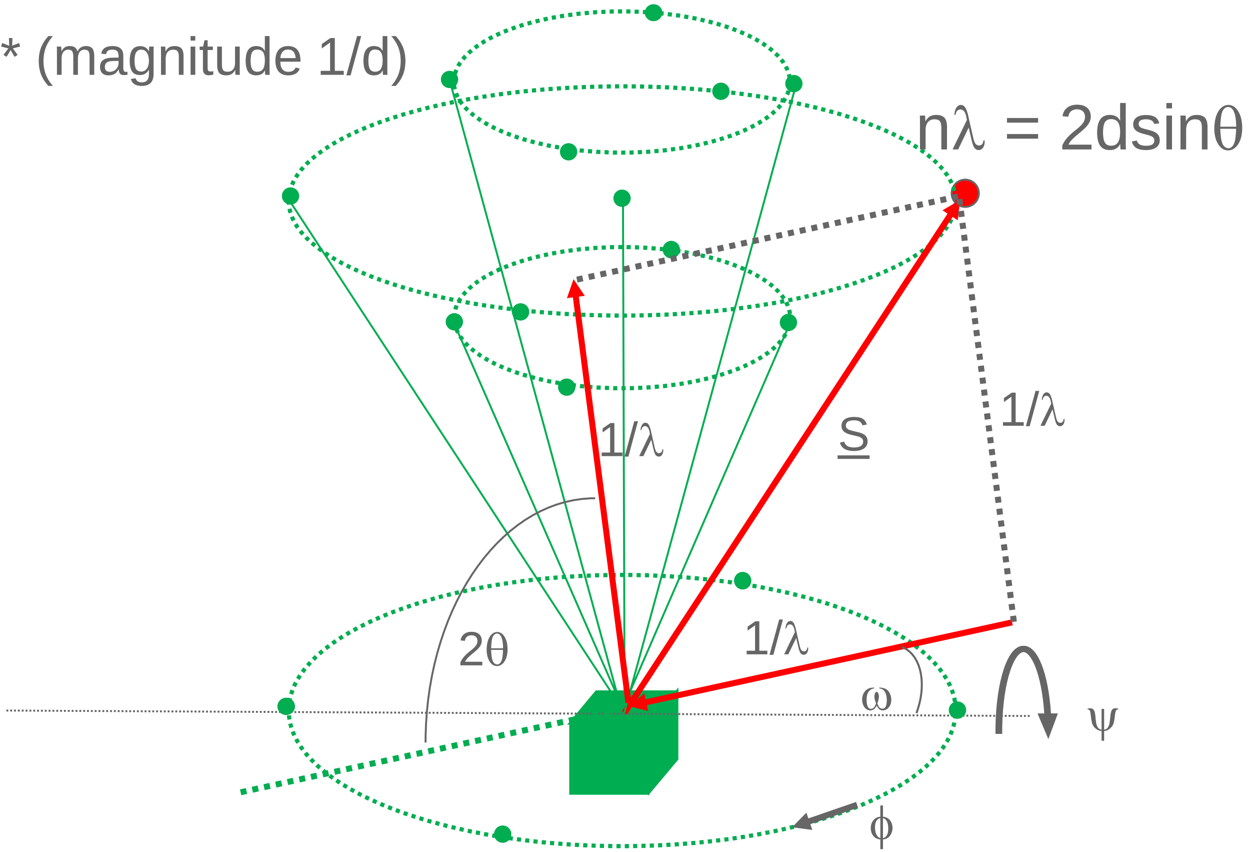

Reciprocal Space Map of Silicon Single Crystal

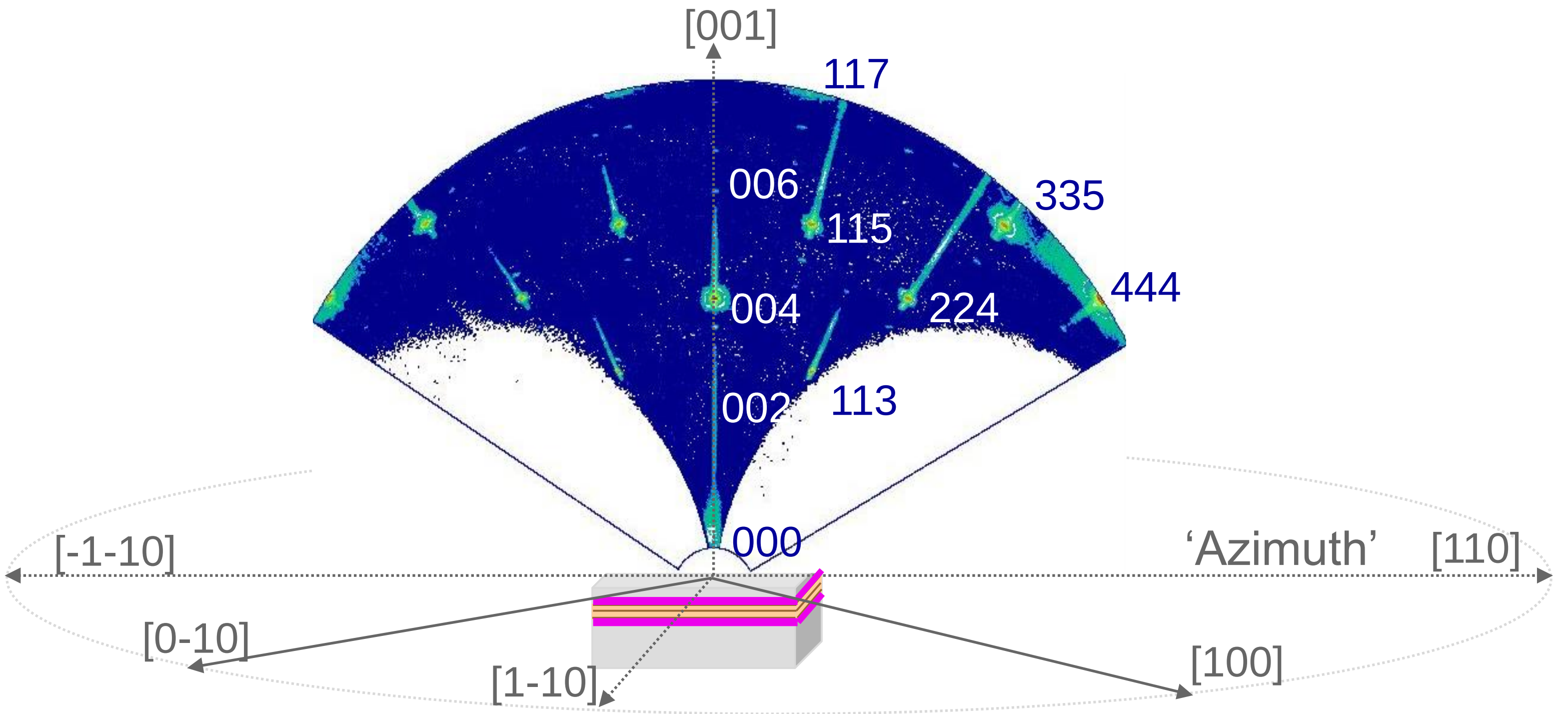

Align the crystal so that the diffraction plane is coincident with a low index plane in the reciprocal lattice (Phi rotation).

Importance of Alignment

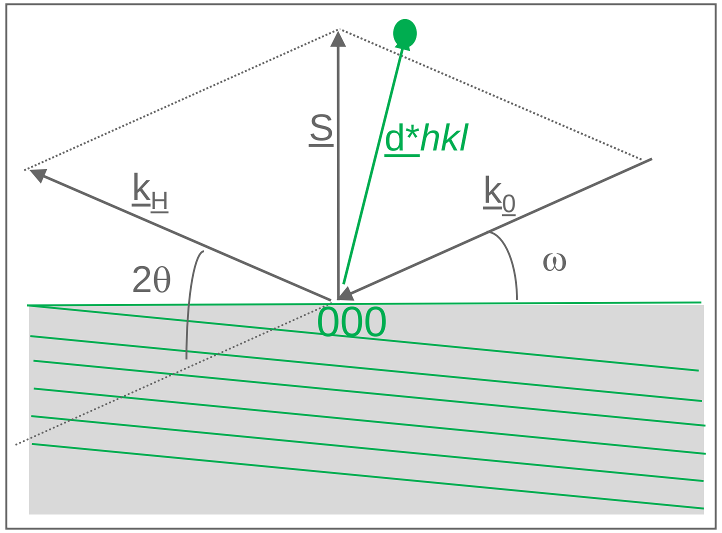

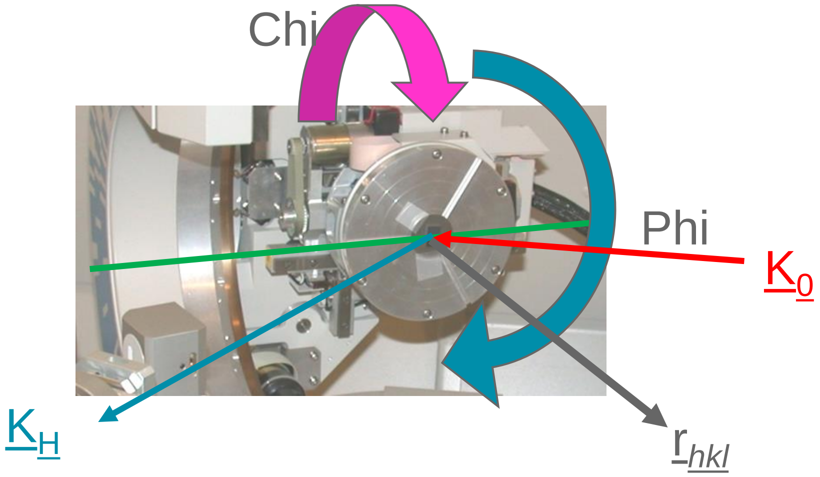

The plane containing $\underline{K}_0$ and $\underline{K}_H$ is called the diffraction plane.

- Phi and Chi are used to bring $\underline{d^*}_{hkl}$ into the diffraction plane.
- $\omega = 0$ is parallel to the sample surface.
- $2\theta = 0$ is parallel to the sample surface.

Reciprocal Space of a Polycrystalline Sample

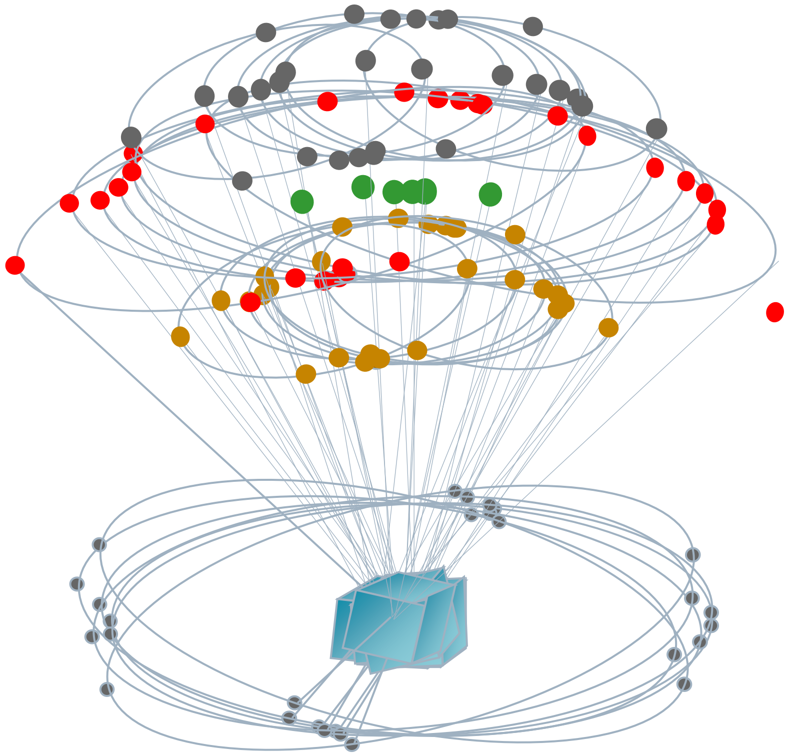

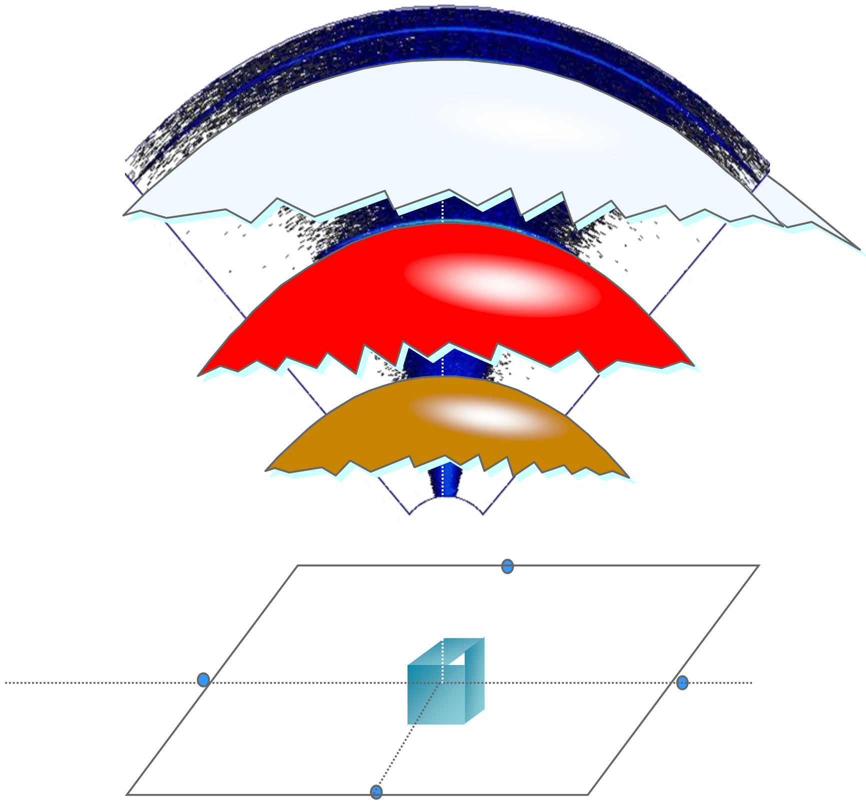

The reciprocal lattices of many single crystals at different orientations superimpose.

Comparing Polycrystalline and Single Crystal Samples

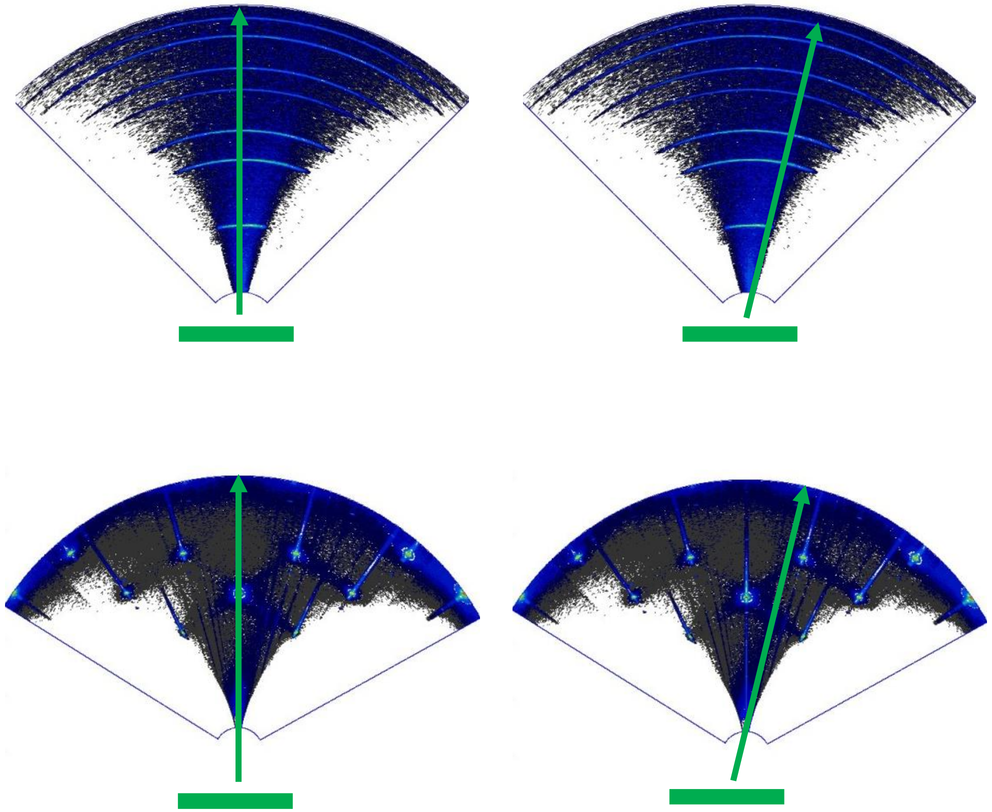

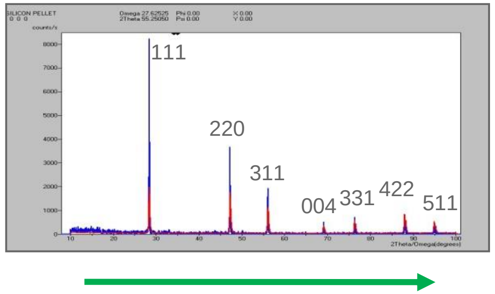

- For polycrystalline Silicon, the same Omega/2Theta scan will be obtained at all orientations of Omega and the same map will be obtained at all Phi and Chi positions.
- For single crystal Silicon, the Omega/2Theta scan will be different at each orientation. Different maps will be observed at different Phi and Chi positions.

Resolution in Reciprocal Space

Low and High Resolution in Reciprocal Space

Si device structure,
Accessible reflections.

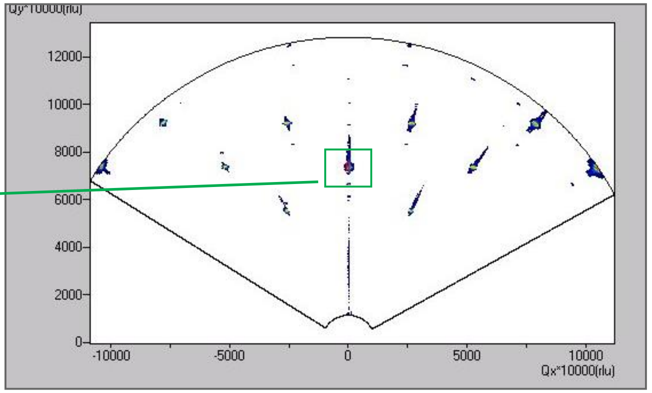

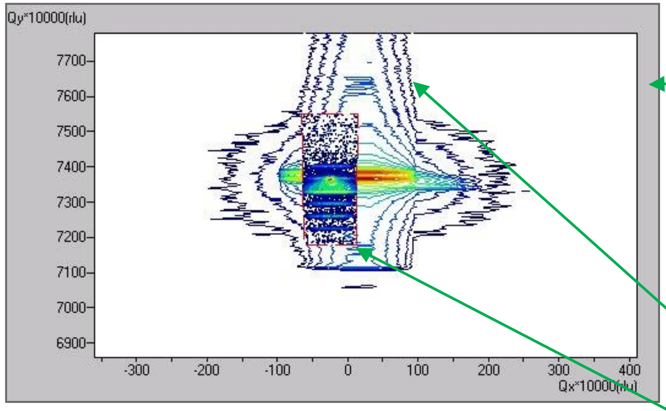

Maps around 004 reflection

- Slit system optics
- Triple axis optics

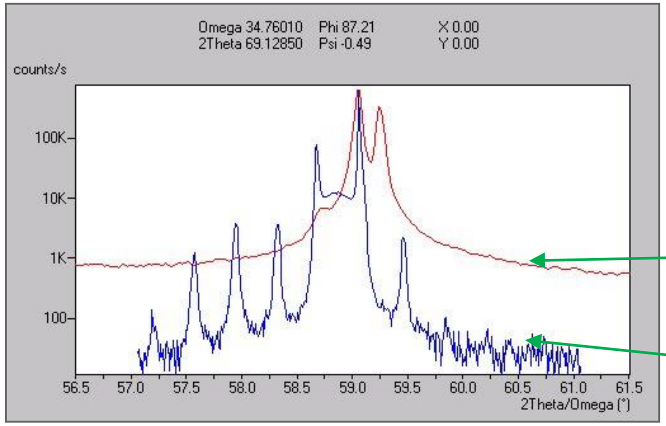

Single Omega/2Theta scans (normalized)

- Slit system optics (Kα_2, high background, smeared features)
- Triple axis optics Omega/2Theta scan

Comparing Scales: Single Crystal Si & Textured Nb/Al

Textured Nb/Al multilayer peak; the size of the Bragg peak is measured in degrees, therefore slit-based optics (e.g. with divergence approx 0.04º) or hybrid + X’Celerator can be used.

Polycrystalline ring

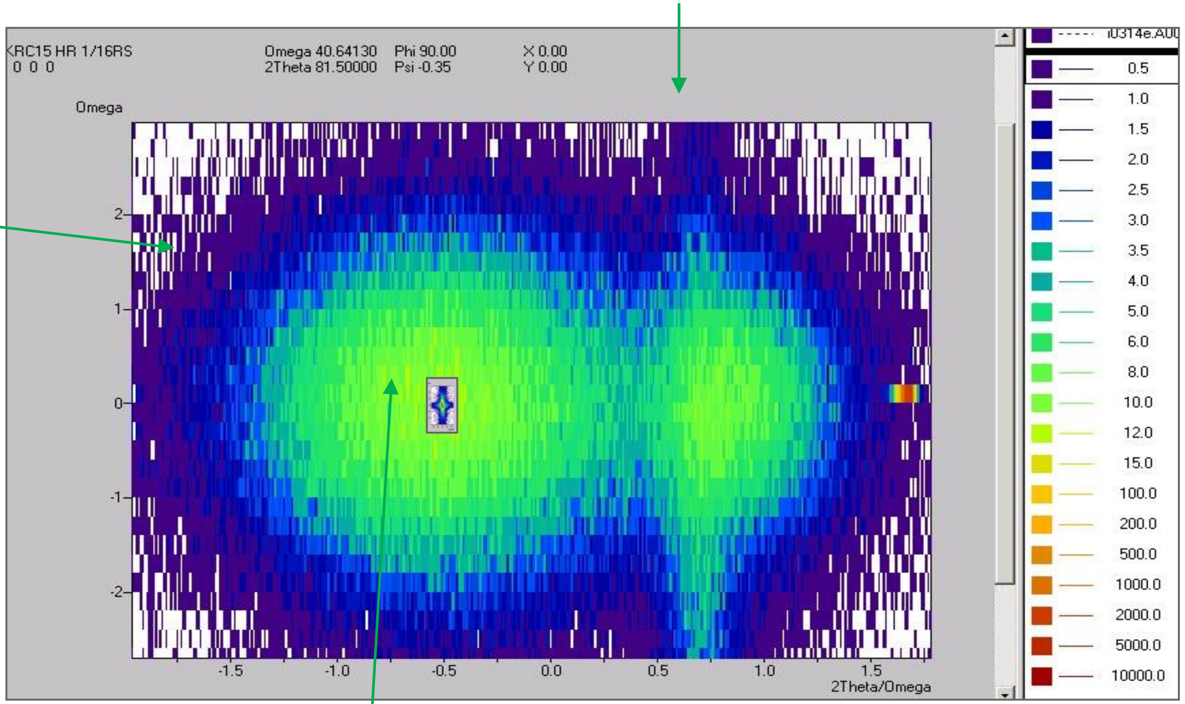

Size of features in single crystal work measured in < 0.01º units, therefore TA optics are required.

Instrument ‘Probe Size’ in Reciprocal Space

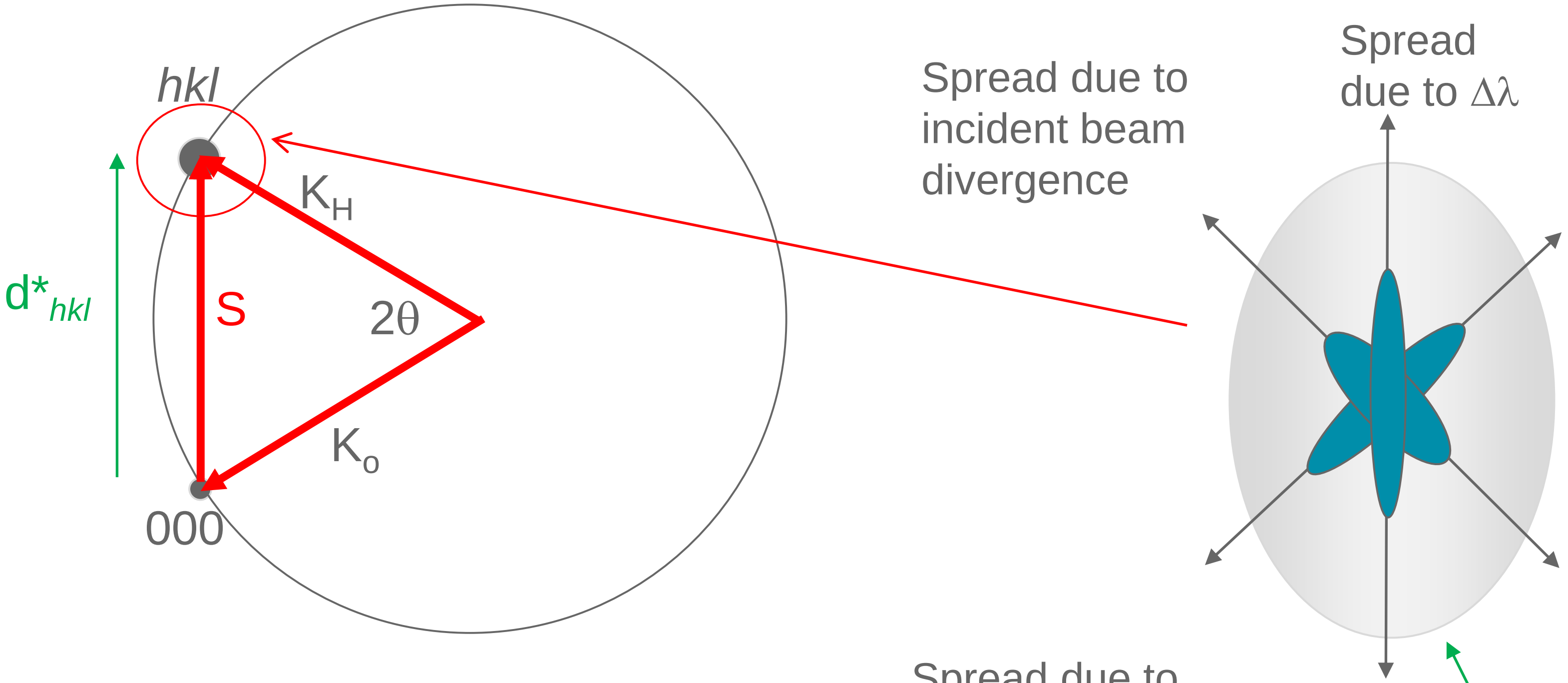

Spread due to incident beam divergence

Spread due to $\Delta\lambda$

Spread due to detector acceptance angle

Reciprocal lattice feature

K_o	incident beam vector
K_H	diffracted beam vector
S	scattering vector
d^*_{hkl}	reciprocal lattice vector

Probe in TA Optics

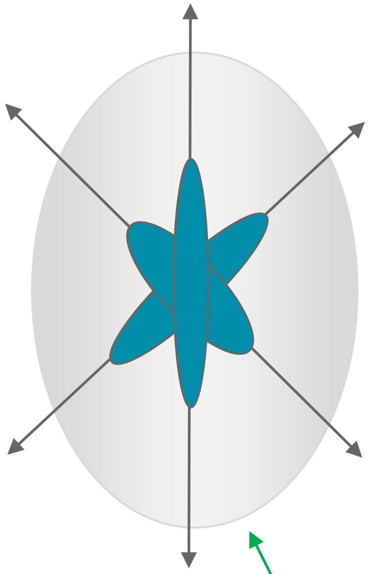

Spread due to incident beam divergence

Spread due to Δλ

Spread due to detector acceptance angle

Reciprocal lattice feature

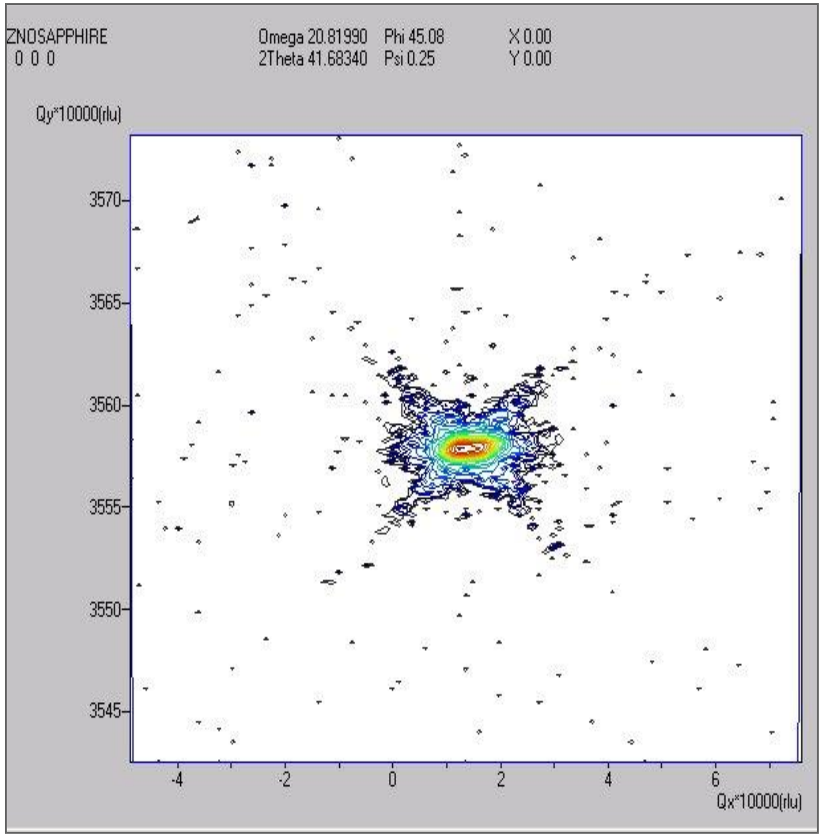

ZNOSAPPHIRE
0 0 0

Omega 20.81990 Phi 45.08
2Theta 41.68340 Psi 0.25

X 0.00
Y 0.00

TA optics single crystal sapphire

Optimizing Step Sizes for Mapping: TA Optics

Consider 2Theta/ω vs ω map around sapphire:

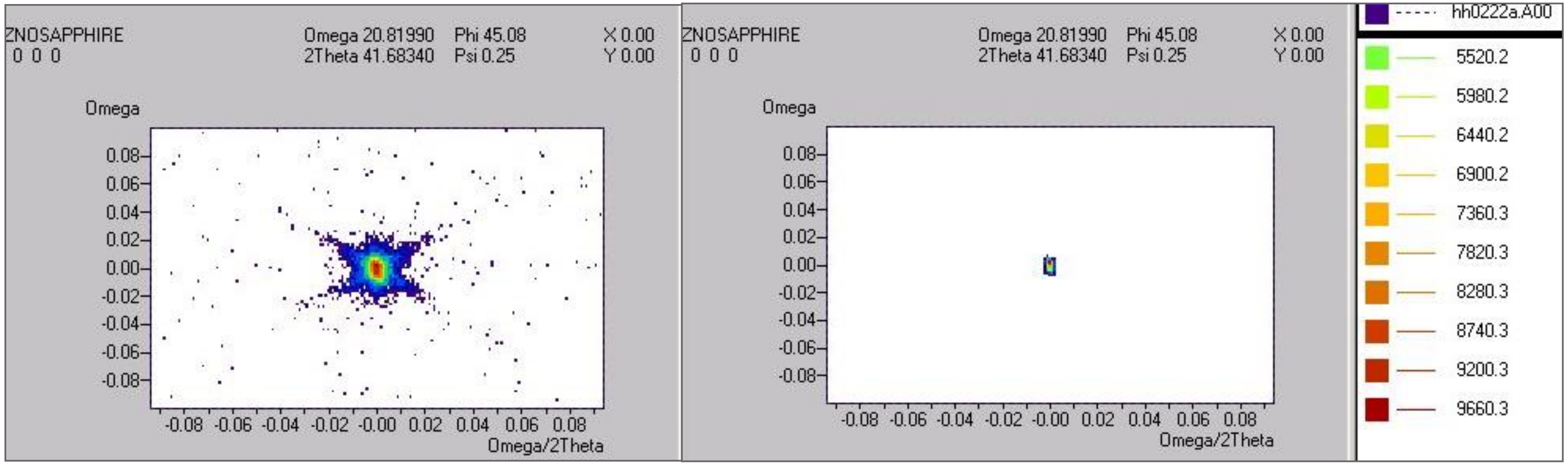

Log scale

Linear scale

Typical scan values: Omega = $0.001 – 0.01^{o}$

Omega/2Theta 0.0005^{o}- 0.005

Probe in Slit Based Optics

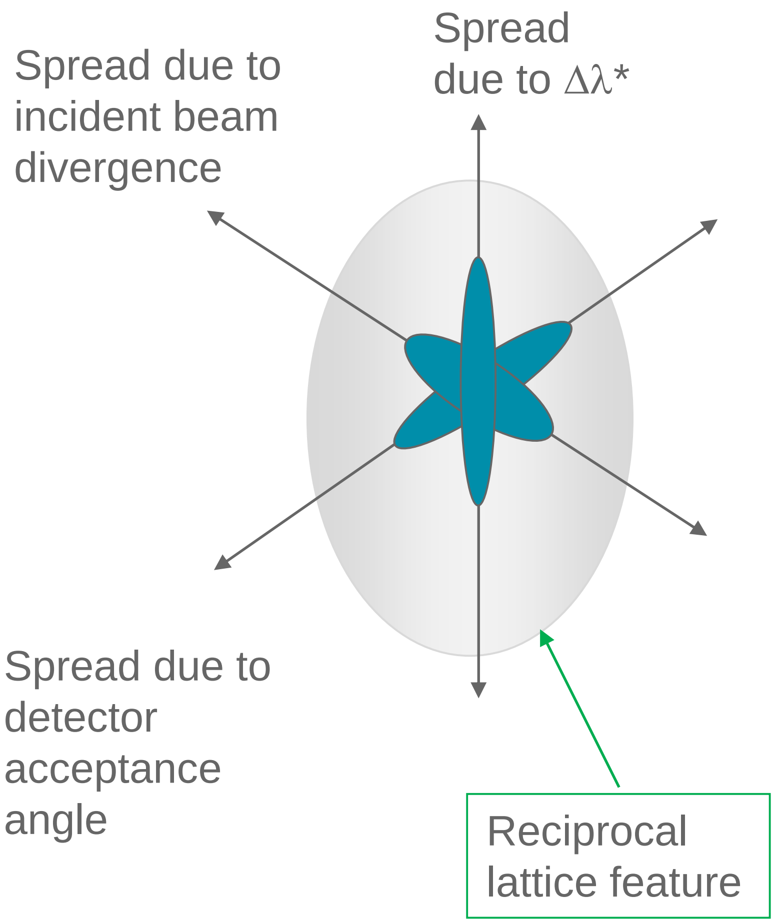

Spread due to incident beam divergence

Spread due to $\Delta\lambda$*

Spread due to detector acceptance angle

Reciprocal lattice feature

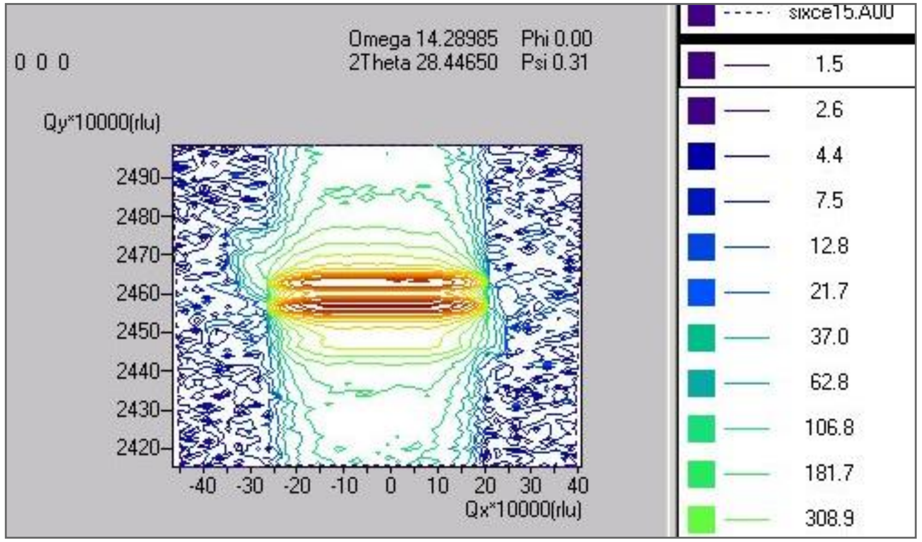

Si 111 peak (Si single crystal sample), 1/32° div. Slit, 5 mask, X'Celerator scanning mode, step size 0.0125°

*Note: $K\alpha_1$ and $K\alpha_2$

Interpreting the Data in Rea and Reciprocal Space

Comparing Map Display Types

004

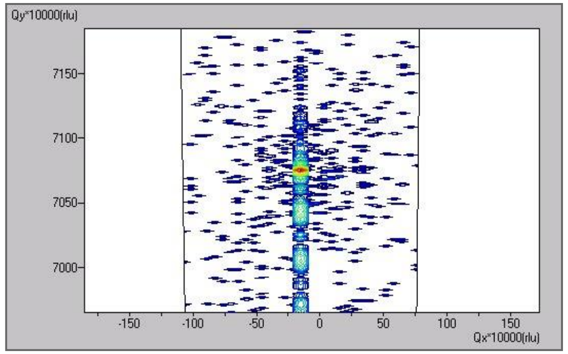

Omega/2Theta x Omega

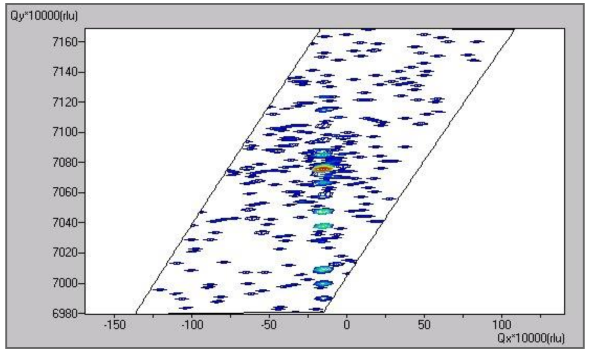

2Theta x Omega

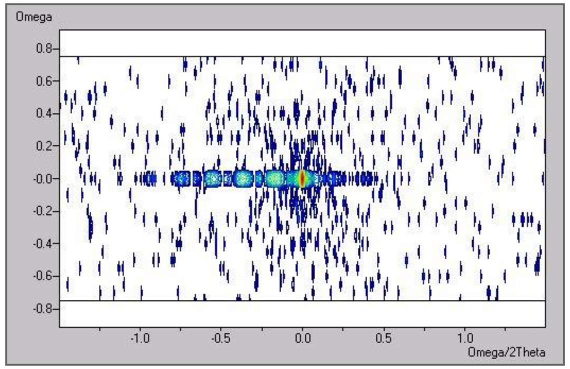

Omega/2Theta x Omega

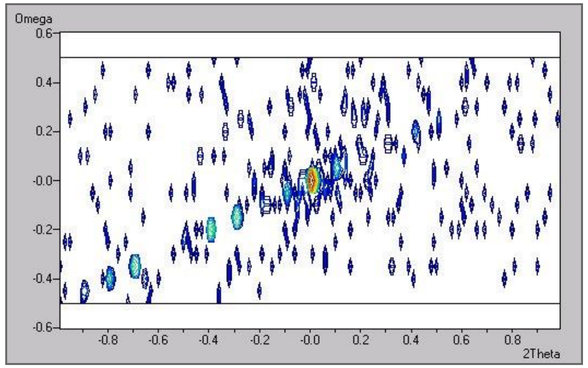

2Theta x Omega

Reciprocal Space Units

- Pattern stays true to sample reciprocal lattice irrespective of type of scan
- Good for interpretation of general features

Angular units

- Pattern orientation is determined by type of scan.
- Good for information about scan dimensions, resolution.

Diffraction Pattern Repeated for Each Reciprocal Lattice Spot

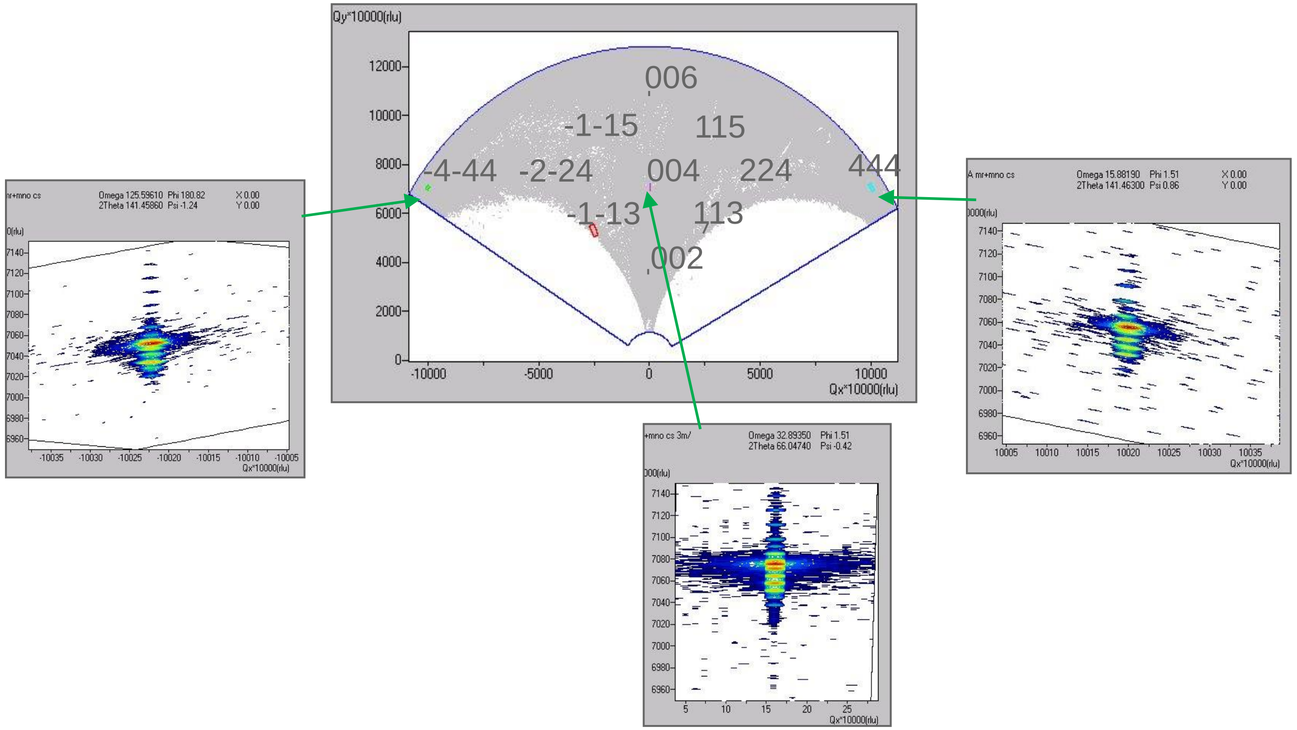

- The whole sample consists of a single crystal.
- The geometry of the structure gives rise to an interference pattern which is repeated in every Bragg peak.
- The pattern can be modeled using dynamical diffraction theory.

Fine Detail in Each Reciprocal Lattice Spot

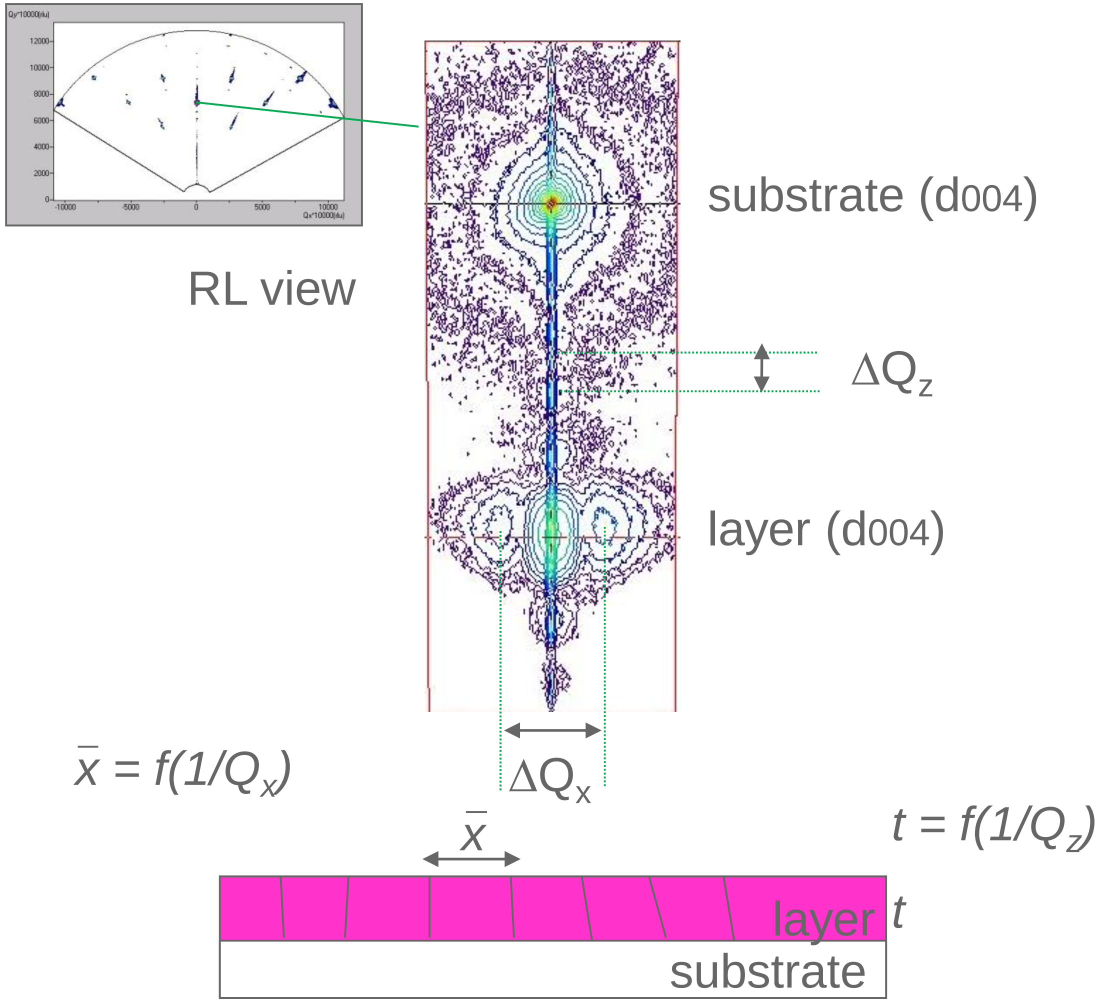

RL view

substrate (d004)

ΔQ_z

layer (d004)

$\bar{x} = f(1/Q_x)$

ΔQ_x

$\bar{x}$

$t = f(1/Q_z)$

layer t

substrate

- The fine details within a reciprocal lattice spot are a function of the shape and size of the perfectly scattering (coherent) region(s) in the crystal.
- Lengths on the reciprocal space map have a reciprocal relationship to lengths in real space

Simulation of Rocking Curves Using Dynamical Diffraction Theory

Dynamical Diffraction Theory: Single Crystals

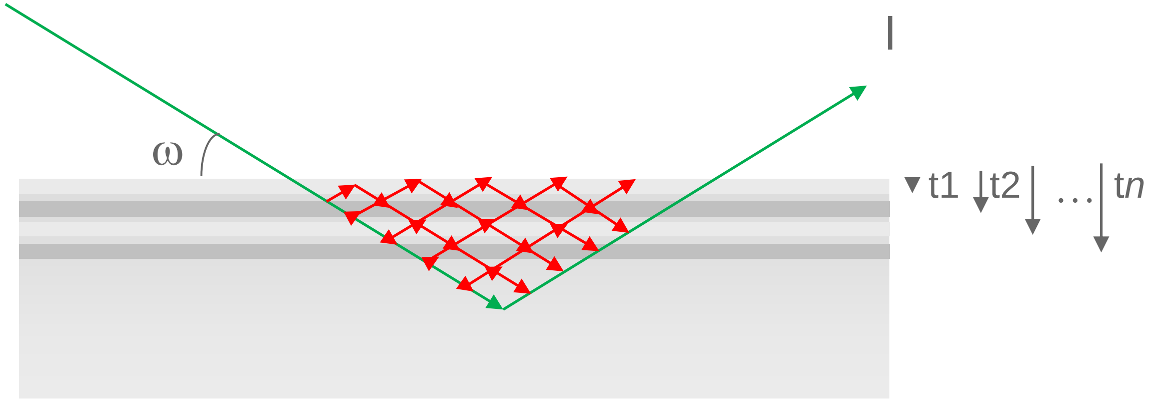

A major feature in the dynamical diffraction theory is that the wave-front is coherent throughout the entire sample volume.

- The effects of lattice defects must be negligible.
- Dynamical effects such as extinction (thickness fringes) become important.

The output intensity (I) is calculated for each angle of incidence (ω), solving boundary conditions at each layer interface (t*n*).

Kinematic Theory: Polycrystalline

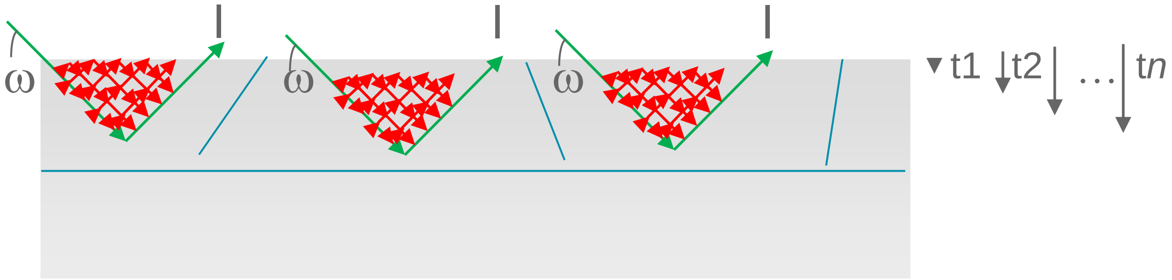

- The kinematic theory is based on the idea that small regions scatter coherently.
- The scatter from each region does not interfere with that from other regions.
- The intensities are simply additive.
- The size of the feature in reciprocal space is inversely related to the thickness of the scattering grain or mosaic block.

Example Material: Semiconductor Device Structure - InGaAs/GaAs

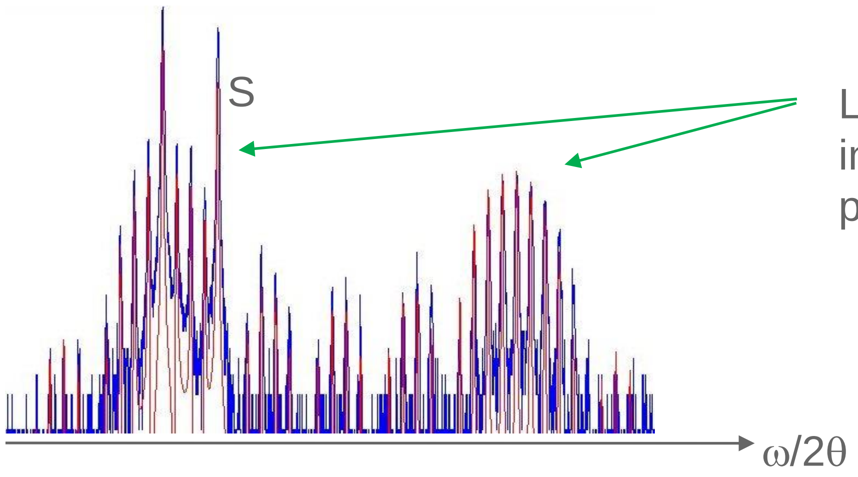

L_1 & L_2 interference pattern

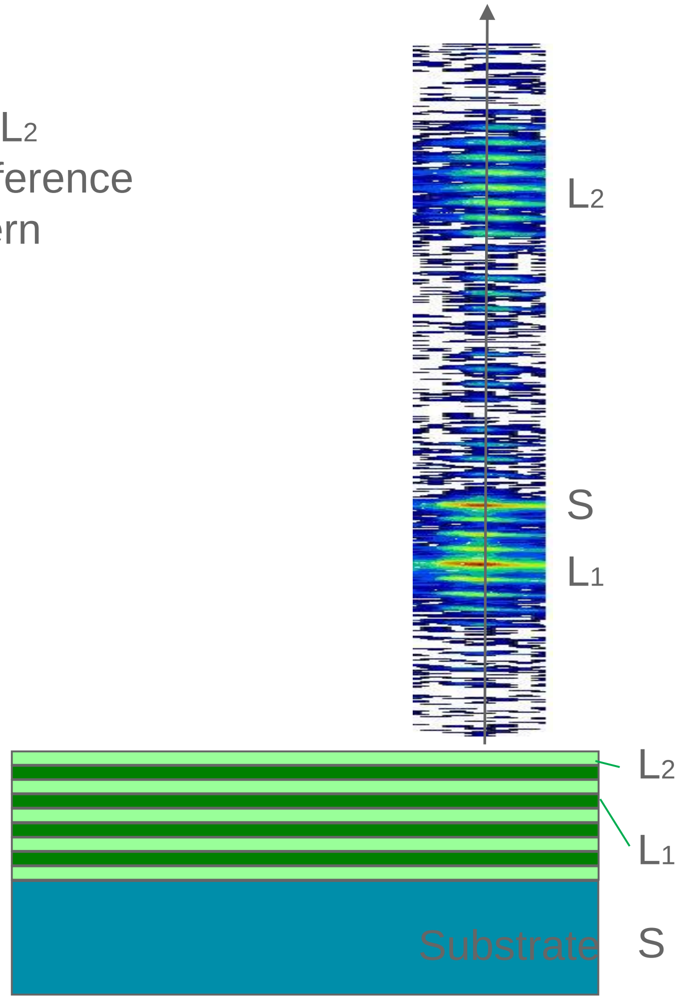

- For a perfect device structure nearly all of the useful information can be obtained from a single scan or rocking curve.
- Simulation of the rocking curve can be used to obtain information such as layer thickness and composition.

Perfect Epitaxial Layer Stack

Substrate Peak

Dynamical interference pattern from finite thickness and periodic multilayer effects

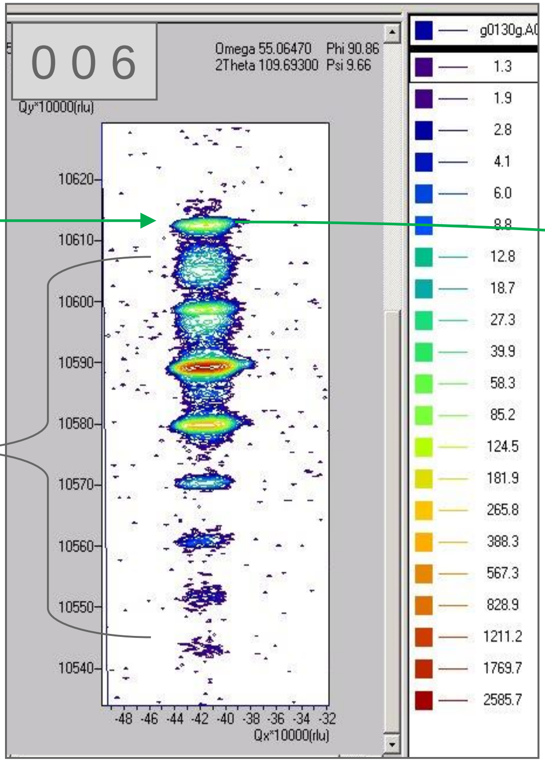

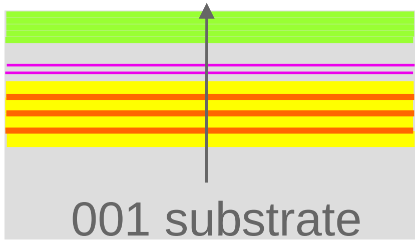

e.g. opto-electronic components (prior to processing):

- Lasers LEDs
- Transistors, integrated circuits

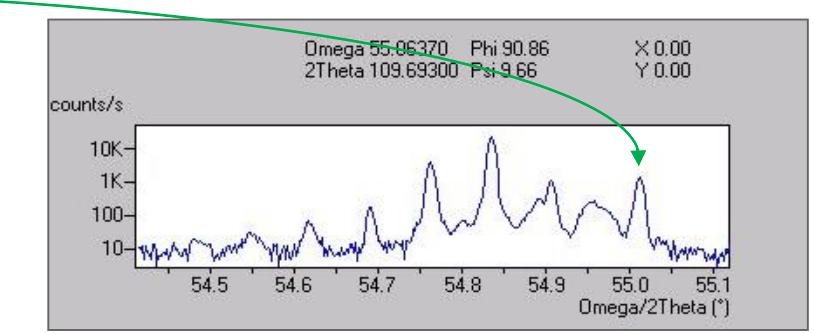

Simulation of the scan through the reciprocal lattice feature provides depth information.

Multilayered structure:

- Layer thicknesses (from Å to µm)
- Alloy compositions - *d*-spacings - strain

NO LATERAL INHOMOGENEITY

Example Materials: Samples with Bend or Tilt

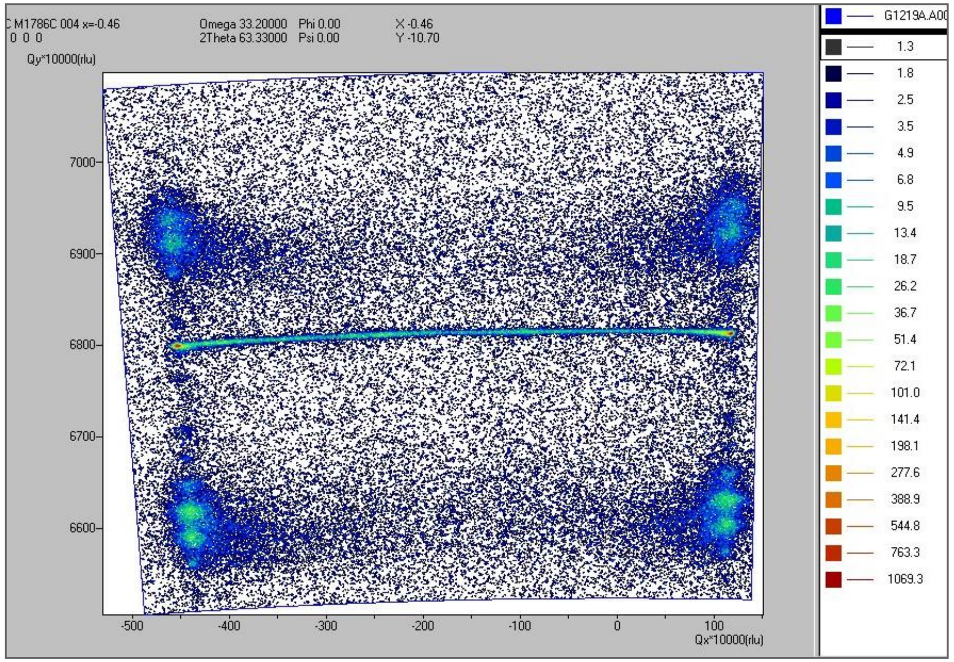

InGaAs tensile and compressive alternating multilayer on 001 InP substrate.

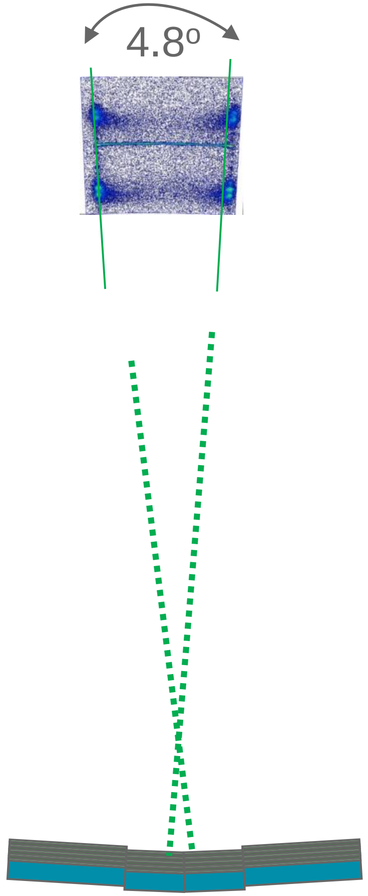

Bent multilayer sample

Notes

- There are many publications in the literature:
  - The theory used in the code for X'Pert Epitaxy 4 is described in Chapter 2, and references therein:

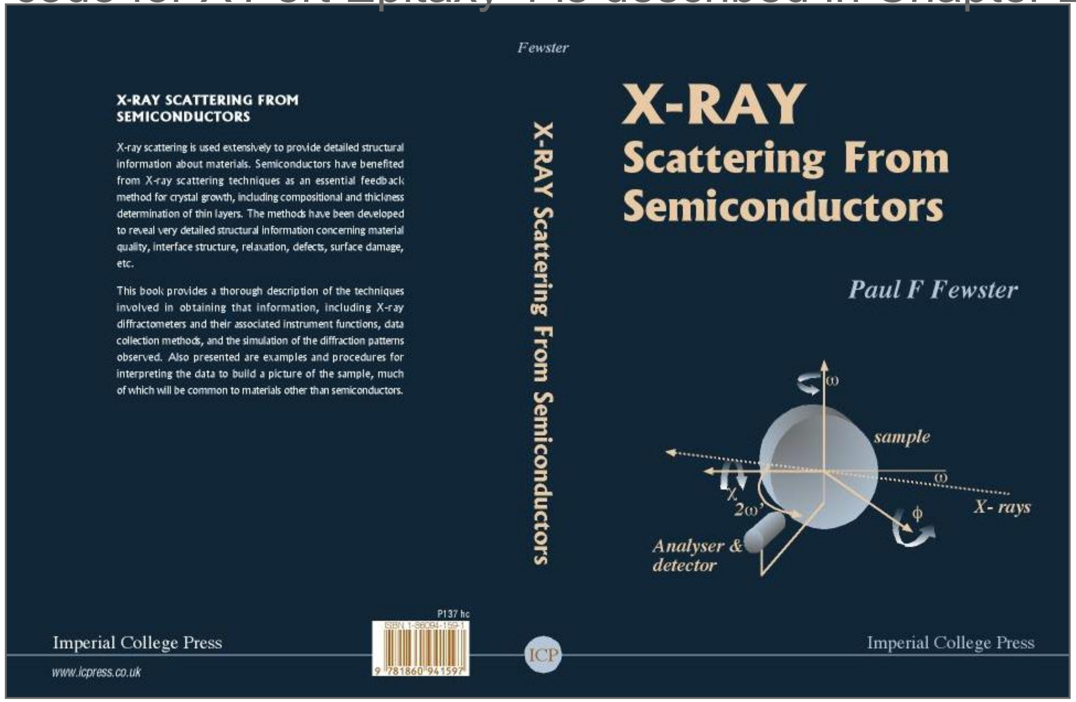

X-RAY SCATTERING FROM SEMICONDUCTORS

X-ray scattering is used extensively to provide detailed structural information about materials. Semiconductors have benefited from X-ray scattering techniques as an essential feedback method for crystal growth, including compositional and thickness determination of thin layers. The methods have been developed to reveal very detailed structural information concerning material quality, interface structure, relaxation, defects, surface damage, etc.

This book provides a thorough description of the techniques involved in obtaining that information, including X-ray diffractometers and their associated instrument functions, data collection methods, and the simulation of the diffraction patterns observed. Also presented are examples and procedures for interpreting the data to build a picture of the sample, much of which will be common to materials other than semiconductors.

Imperial College Press
www.icpress.co.uk

P137 hc
ISBN 1-86094-159-1

Fewster

X-RAY Scattering From Semiconductors

ICP

X-RAY Scattering From Semiconductors

Paul F Fewster

Imperial College Press

ISBN 1-86094-360-8

Calculations of Composition and Relaxation from Peak Positions

Buffer Layer Structures

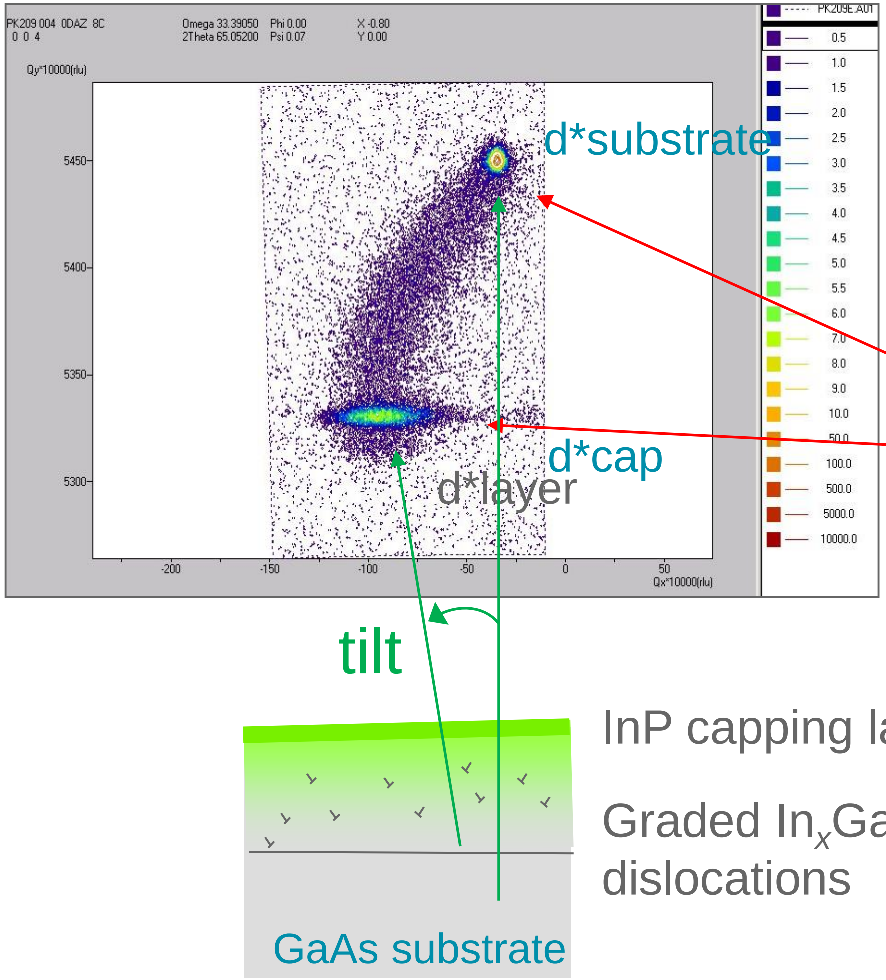

InP capping layer

Graded $In_xGa_{(1-x)}As$ Buffer layer with dislocations

Relaxed Buffer layers as virtual substrates:

e.g. Si/Ge on Si
InGaAs on GaAs
GaN on Sapphire

Substrate and surface layer lattice parameter calculations from reciprocal lattice coordinates (Bragg's Law)

P. Kidd *et al*, J. Crystal growth, (1996) 169 649-659

Example Material: Relaxed Buffer Layer

e.g. InGaAs step graded Buffer Layer with InP cap on 001 GaAs substrate

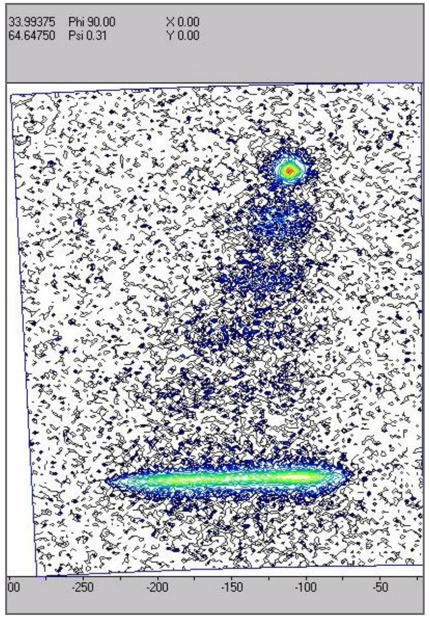

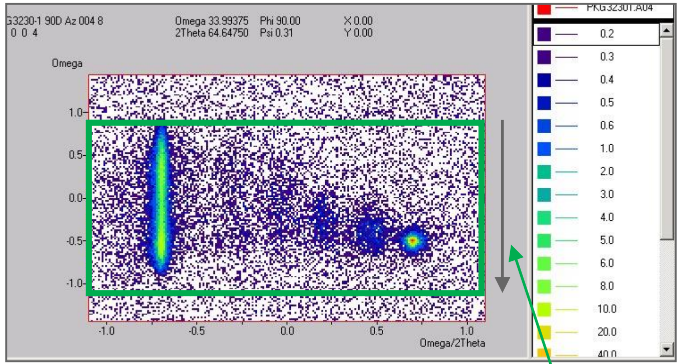

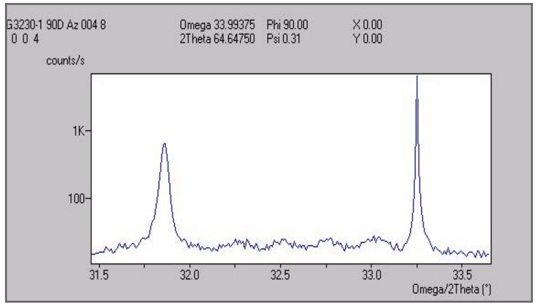

If these files are added together ("projected") then a rocking curve can be obtained in which the peaks from the individual layers are separated.

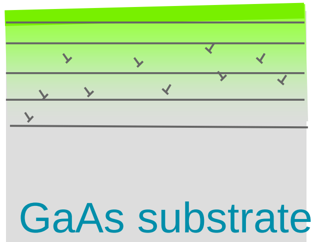

In a conventional rocking curve, collected with an open detector, the peaks would smear into each other and be indistinguishable.

Example Material: Imperfect Device Structure

e.g. InGaN on GaN on Sapphire

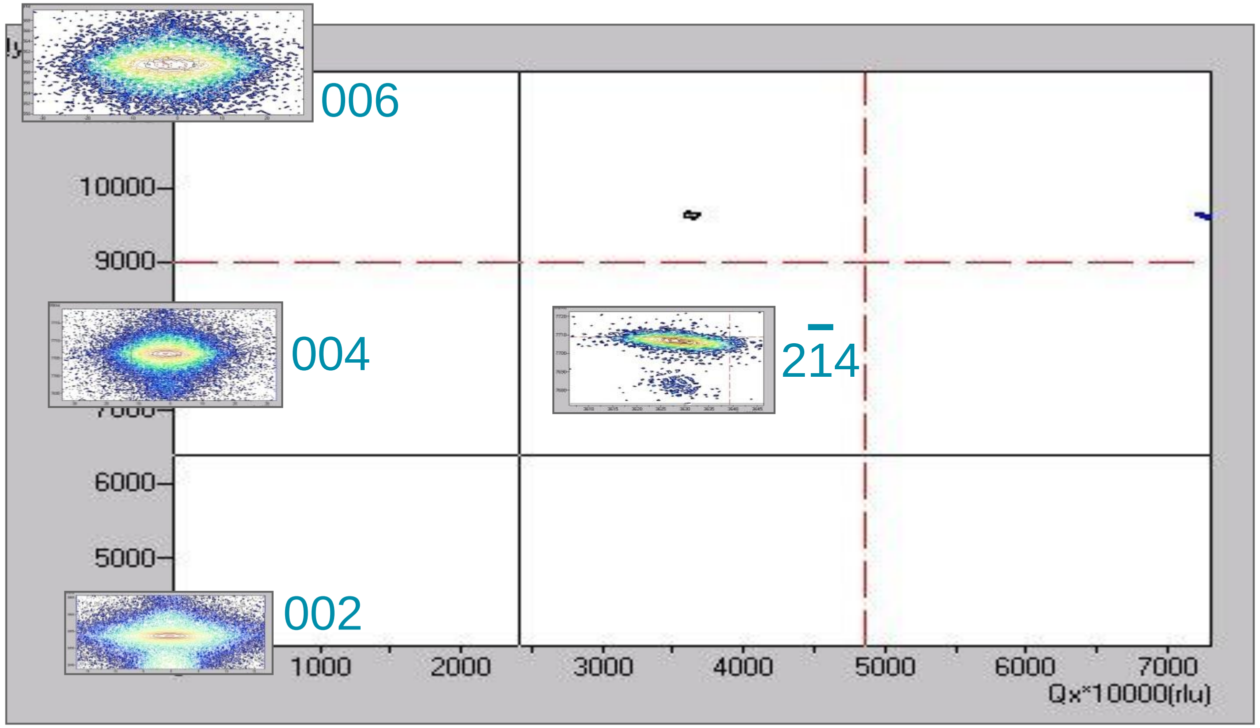

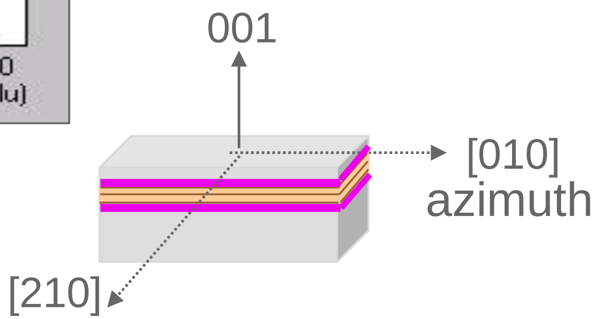

Example Material: Imperfect Device Structure

e.g. InGaN on GaN on Sapphire

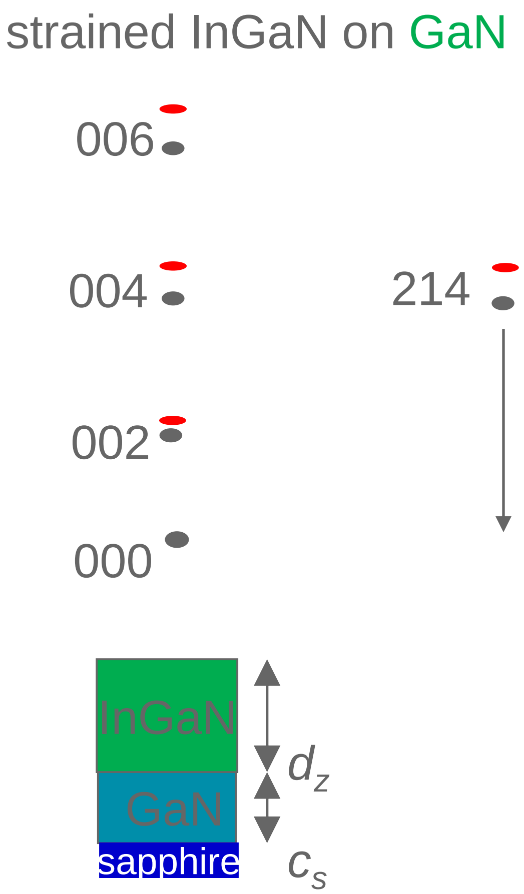

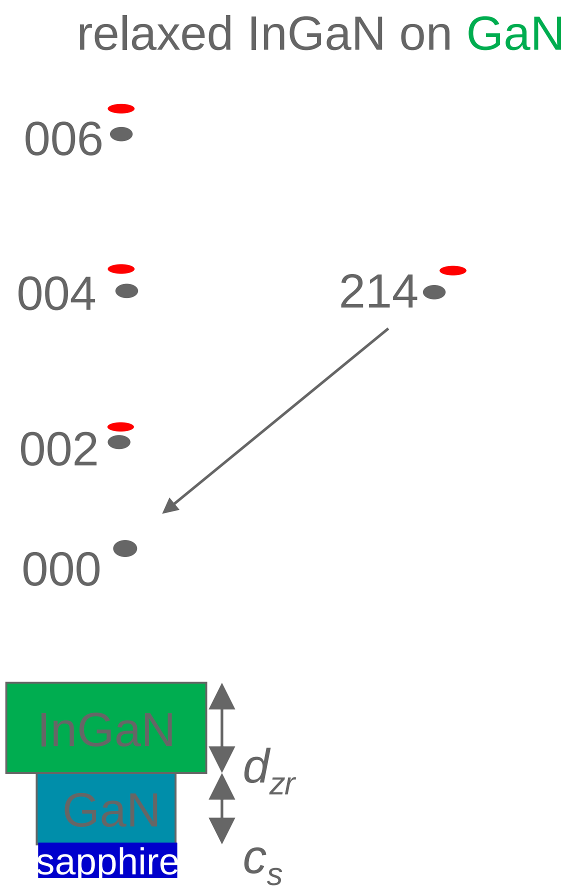

Notes

There are available a number of notes about calculations of composition and relaxation from rocking curves and maps:

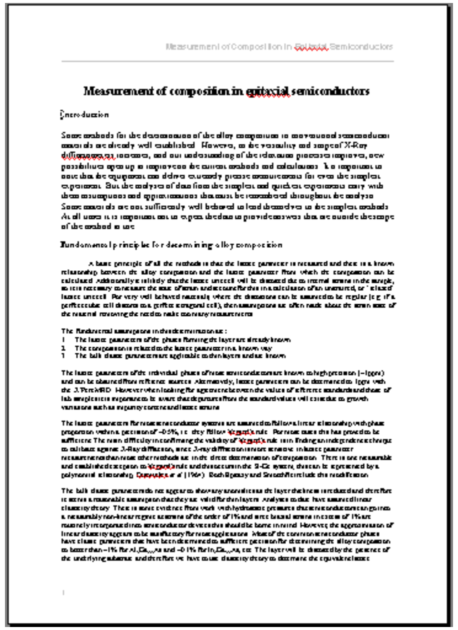

Measurement of Composition in Epitaxial Semiconductors

Measurement of composition in epitaxial semiconductors

Introduction

Fundamental principles for determining alloy composition

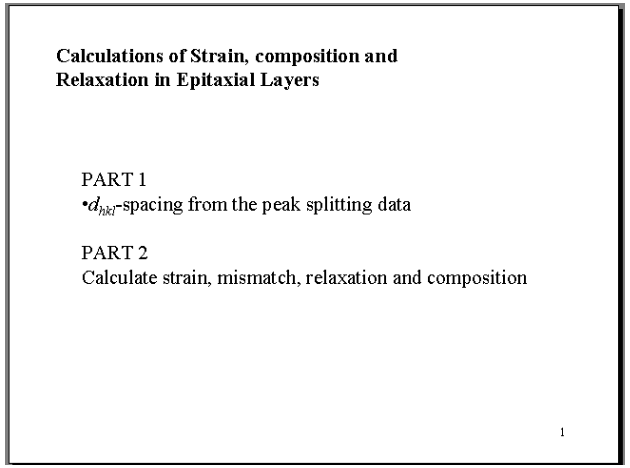

Calculations of Strain, composition and Relaxation in Epitaxial Layers

PART 1

•d_{hkl}-spacing from the peak splitting data

PART 2

Calculate strain, mismatch, relaxation and composition

1

Detailed document:
Measurement of composition and relaxation in semiconductors

Presentation:
Calculations of strain, composition and relaxation in Epitaxial Layers

Lateral Size Effects Observed in Maps

Perfect Devices with Lateral Structure

e.g. Quantum dots, Quantum wires

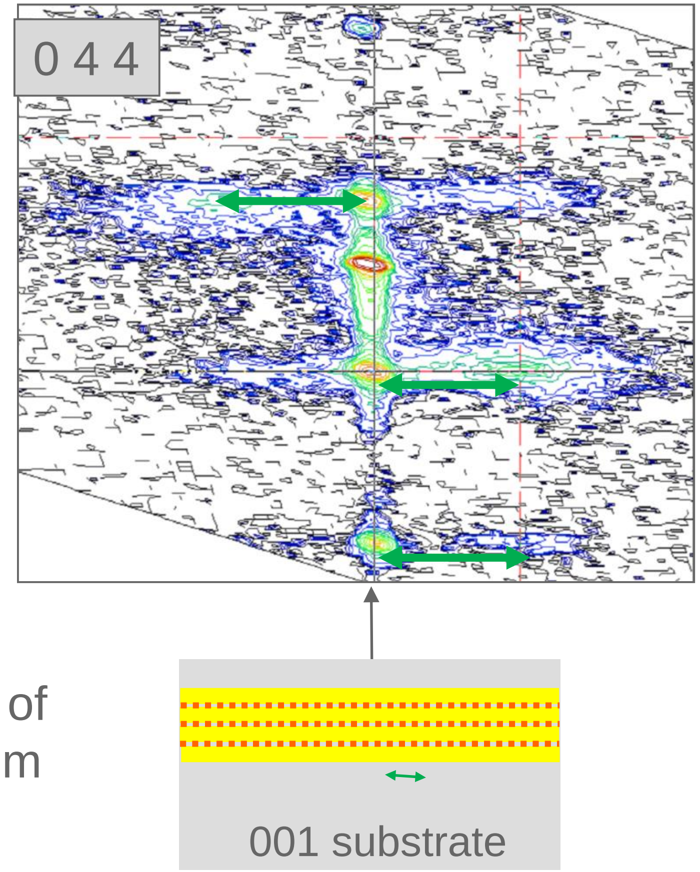

Arrays of quantum dots

Dynamical diffraction theory

Effect of lateral periodicity

Dot spacing ~ 83 nm
Dispersion 67 – 116 nm

P F Fewster, Inst. Phys. Conf. Ser. 164 (1999) p197- 206

Crystallite Size from Reciprocal Space Maps

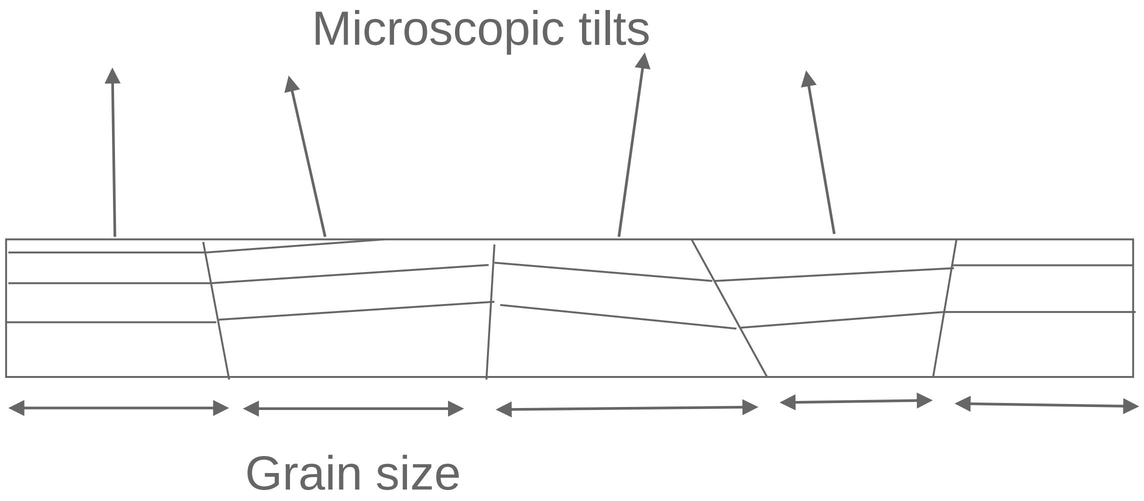

A single crystal will contain some defects. Even though it may scatter with only one Bragg peak, the peak may be spread due to mosaic structure (e.g from dislocation networks). The mosaic structure gives rise to microscopic tilts and finite grain sizes. These can be measured directly from the dimensions of Bragg peaks measured in high resolution reciprocal space mapping.

Spread of Peak: Tilt, Thickness and Lateral Width

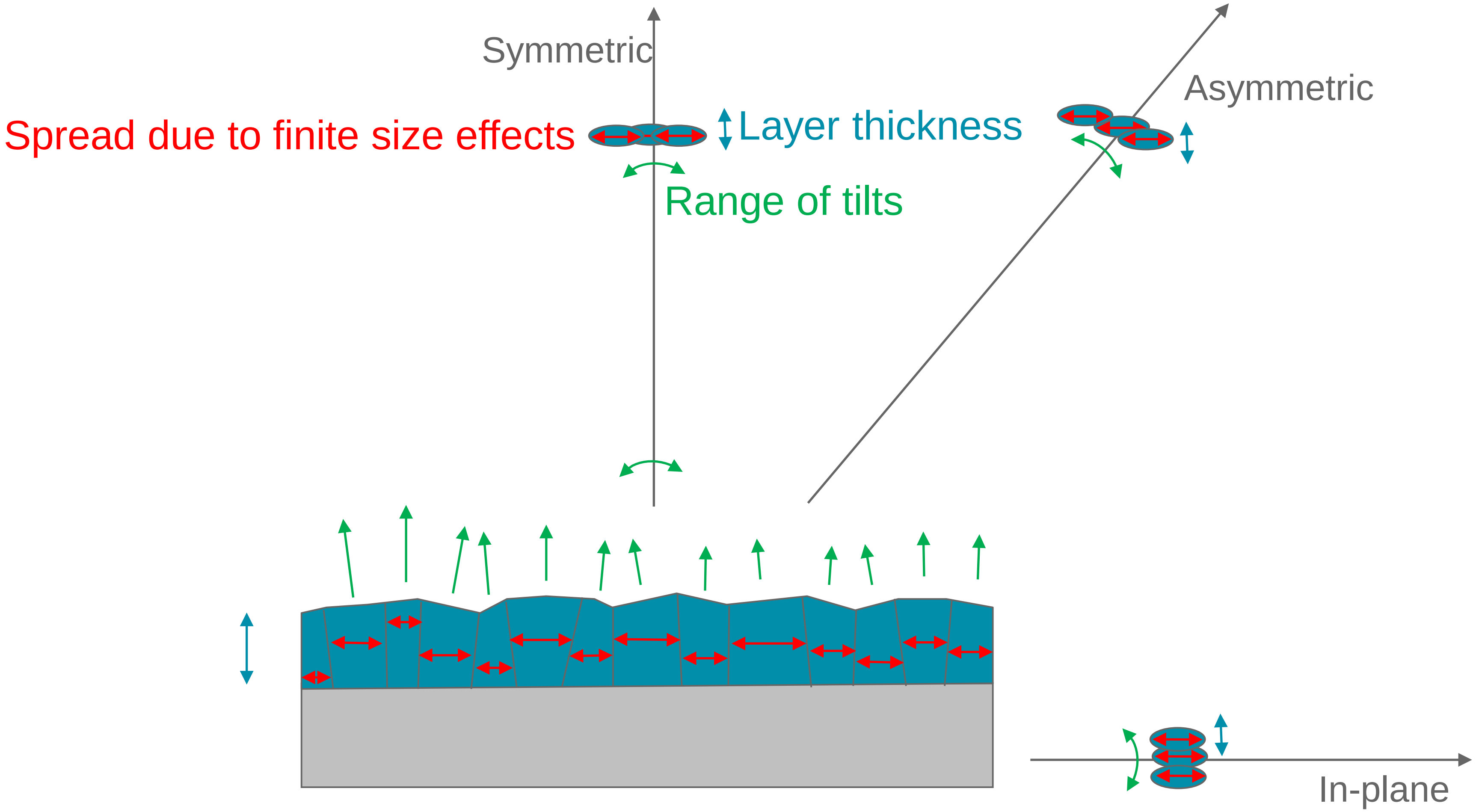

Measure Tilt from Symmetric Reflections in Reciprocal Space

Omega broadening due to tilts

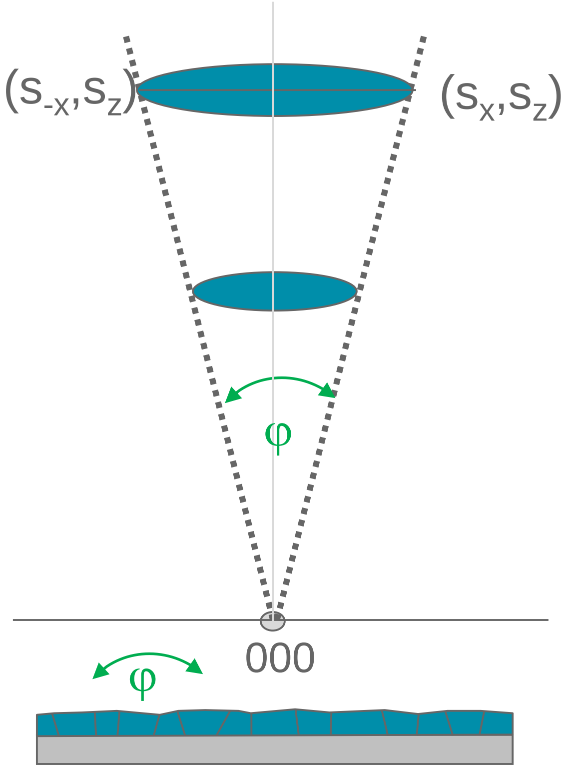

Omega broadening due to size effects

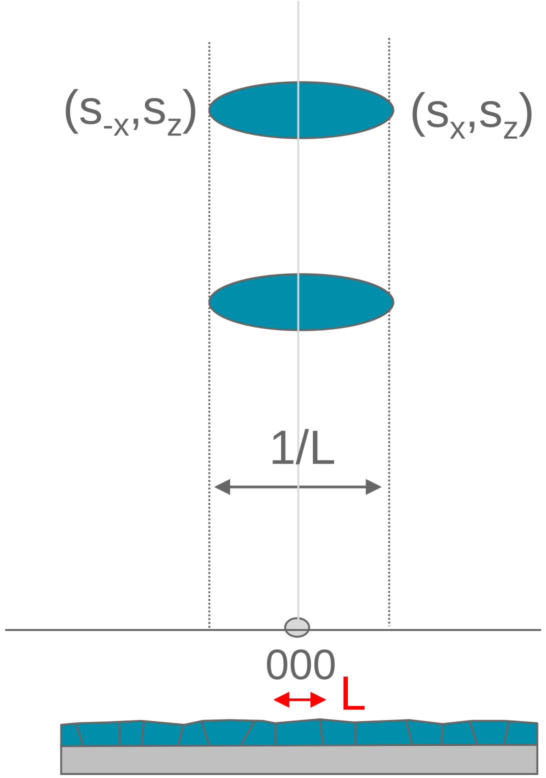

Measure Tilt and Lateral Corr. Length Using Asymmetric Reflections

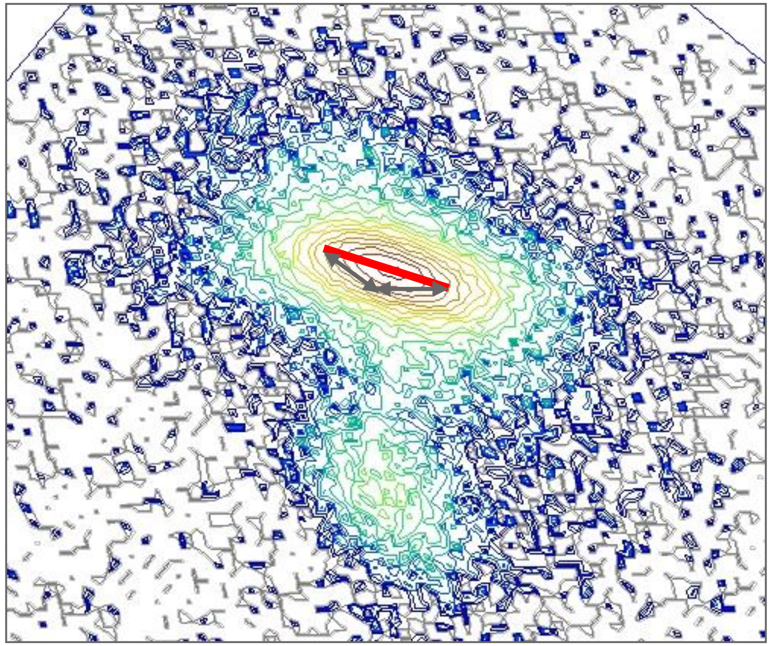

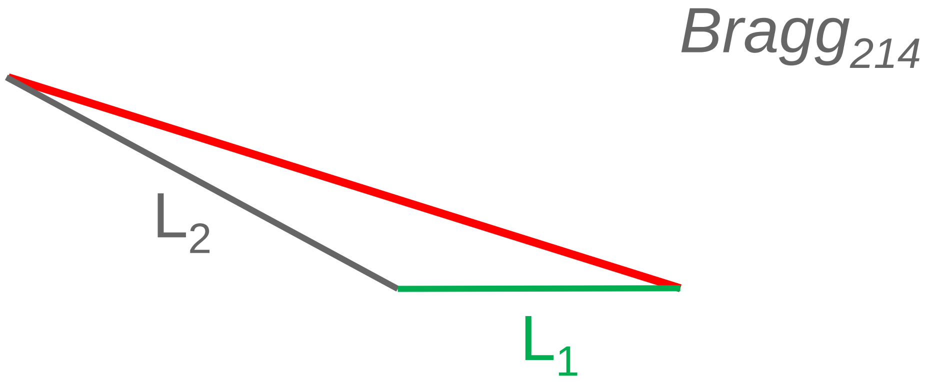

Lateral correlation length $= 1/L_1$ (lateral grain size)
$= 102$ nm

Microscopic tilt $= L_2 / \{ s_x^2 + s_z^2 \}^{1/2}$
$= 0.006^0$

General Observations in Maps to Reveal Microstructure

Reciprocal Space Structure of a Textured Polycrystalline Sample

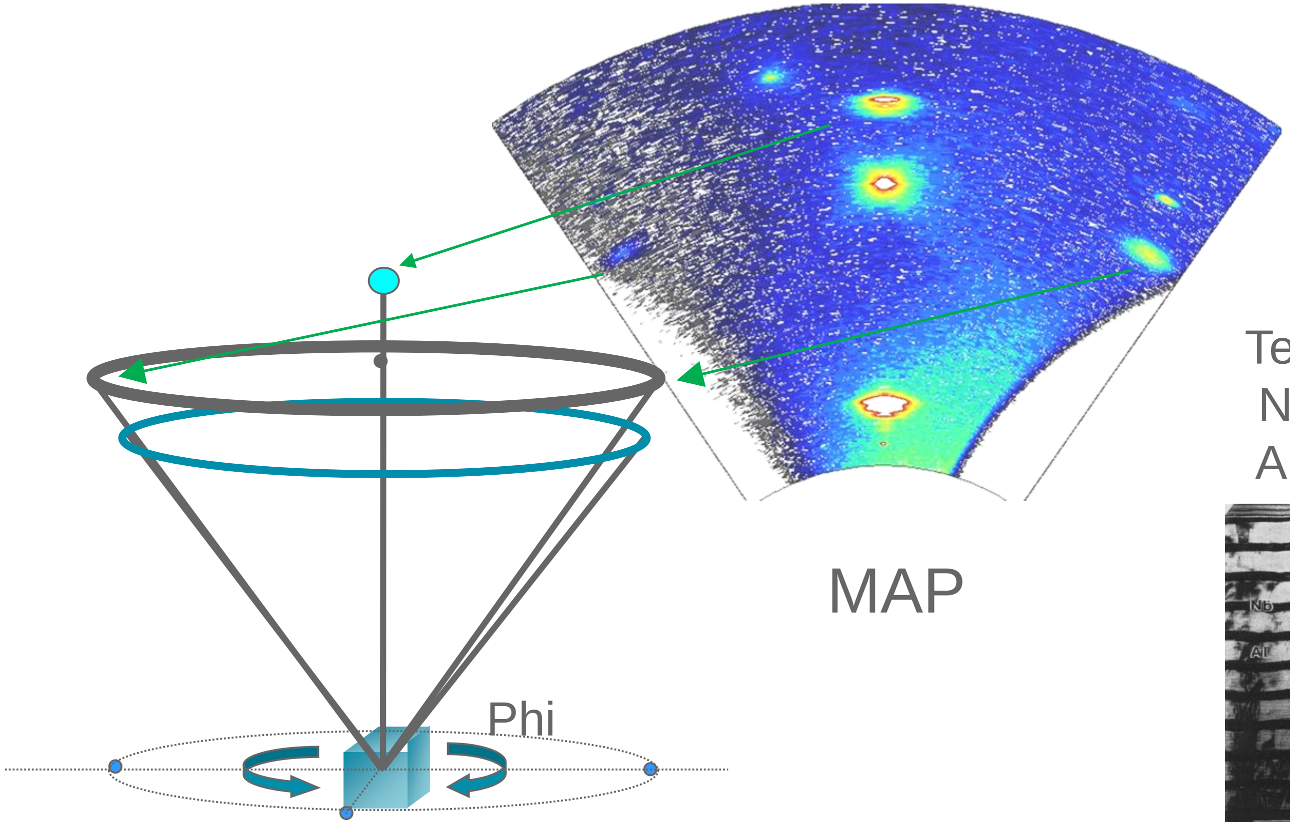

Reciprocal space structure

Textured multilayer
Nb (2.5 nm) –
Al (7.5 nm)

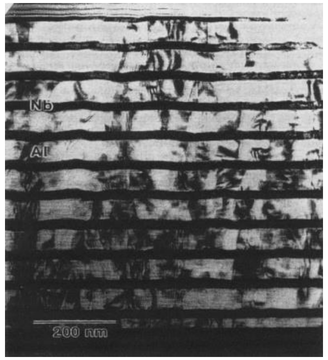

Silicon substrate

Textured Nb-Al Multilayer Thin Films

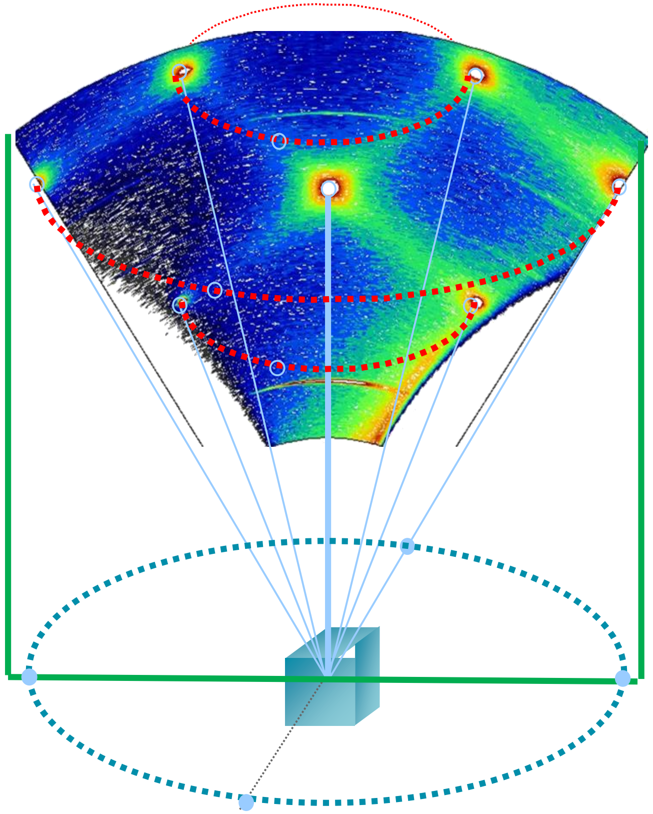

Rotate sample in Phi to include major reflections from substrate

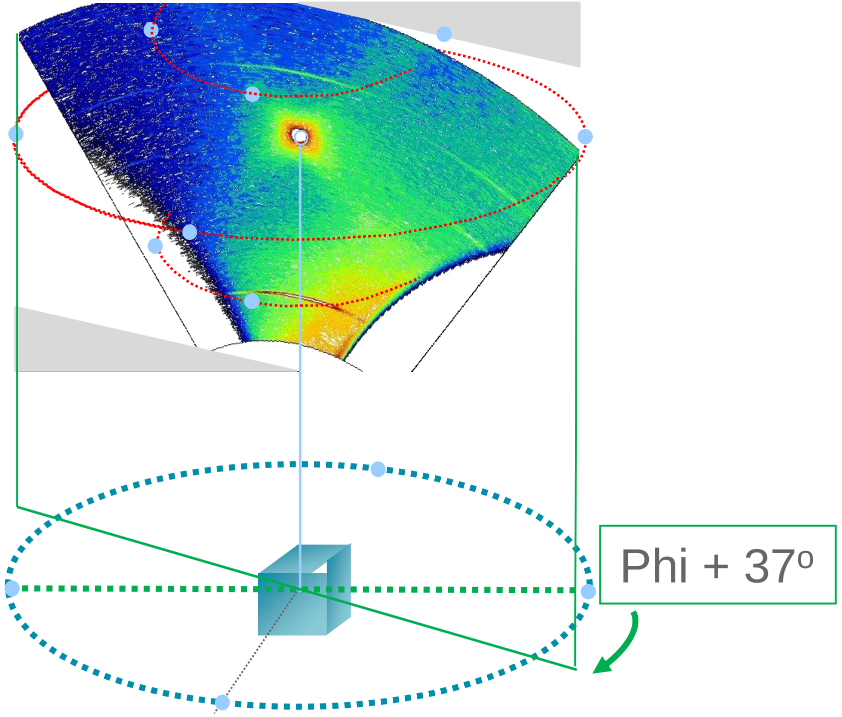

Rotate sample to avoid major reflections from substrate

Texture and Preferred Orientation

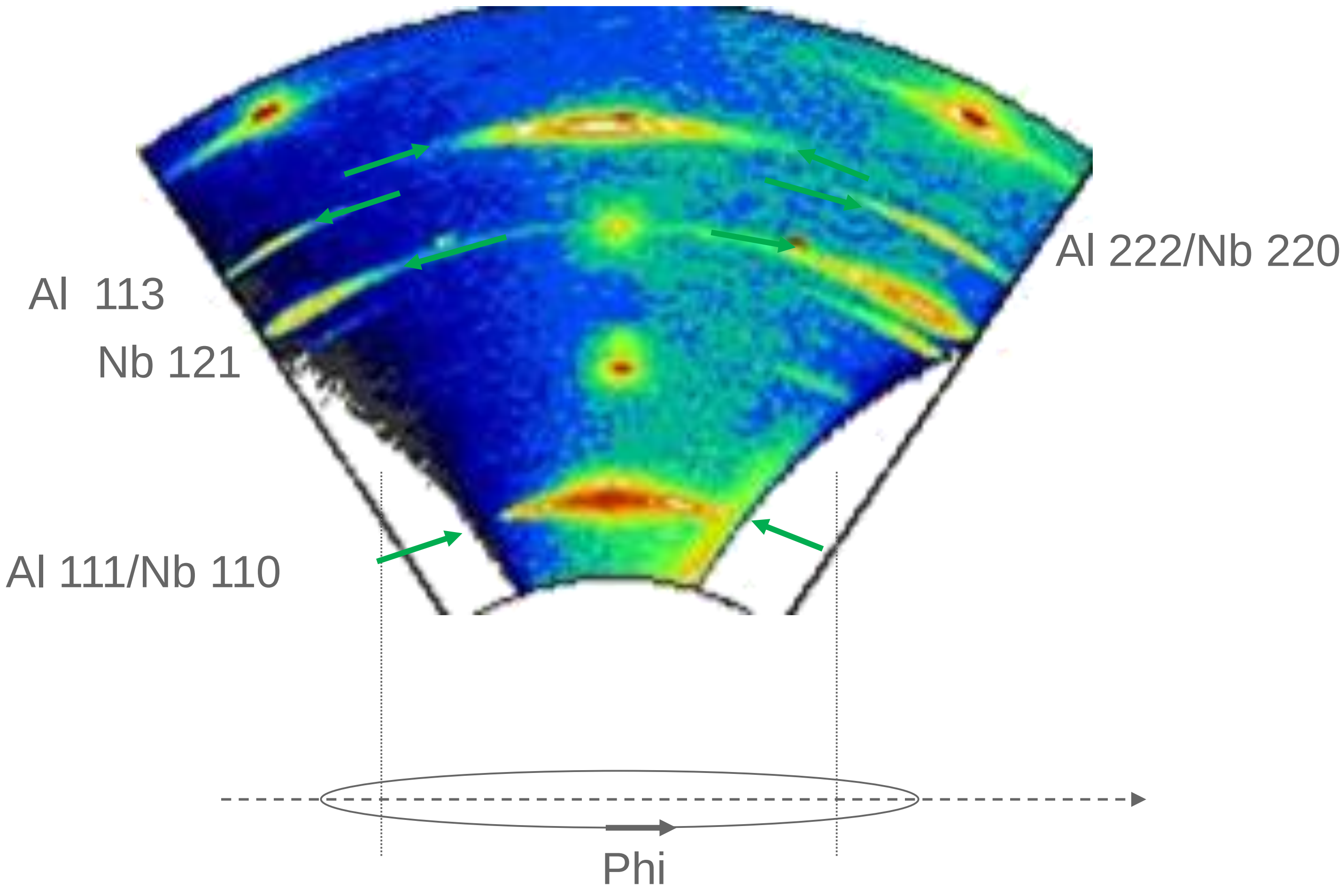

Evidence for Subtle Preferred Orientation?

Development of Strategy:
1) Rotate Phi well away from 110 azimuth Si peak
2) Scan Omega along 113 polycrystalline ring

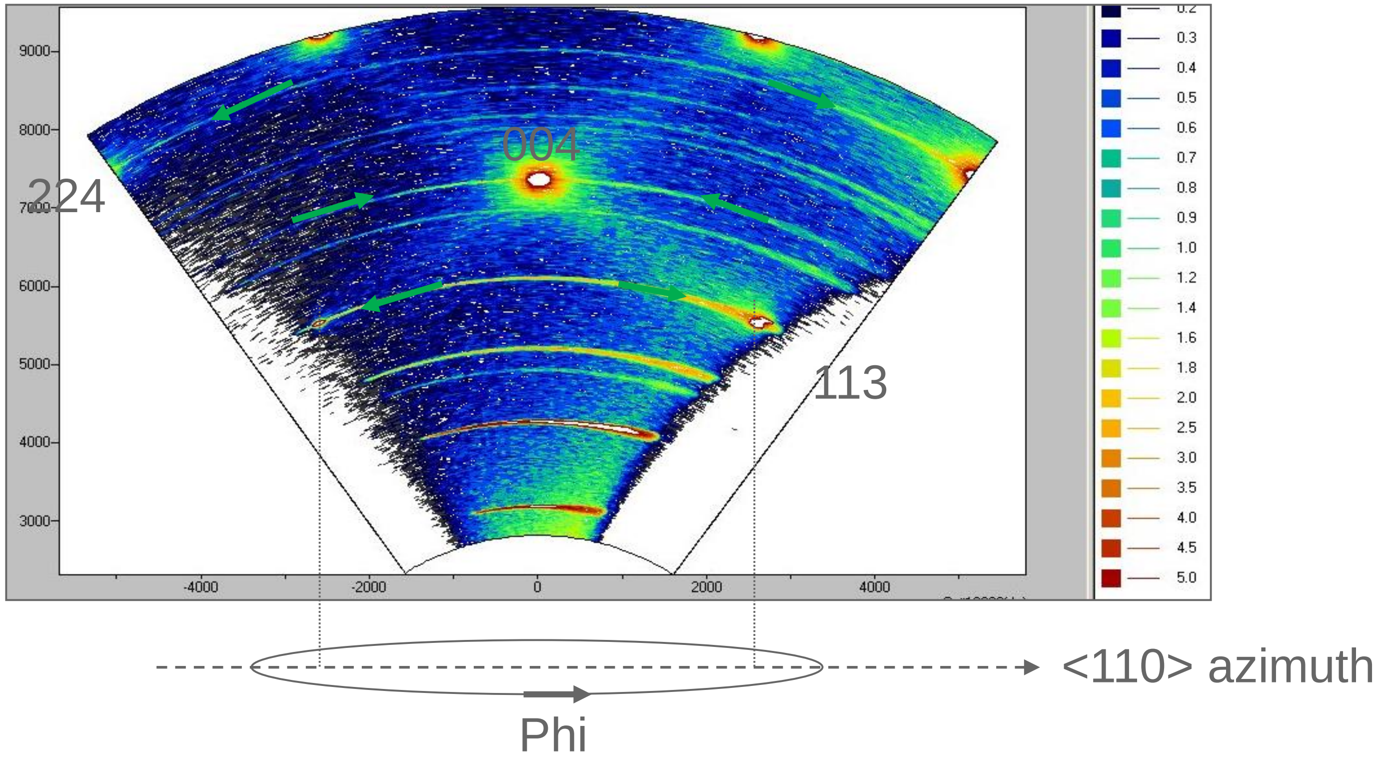

Example Material: Polymer ErQ on Glass Slide

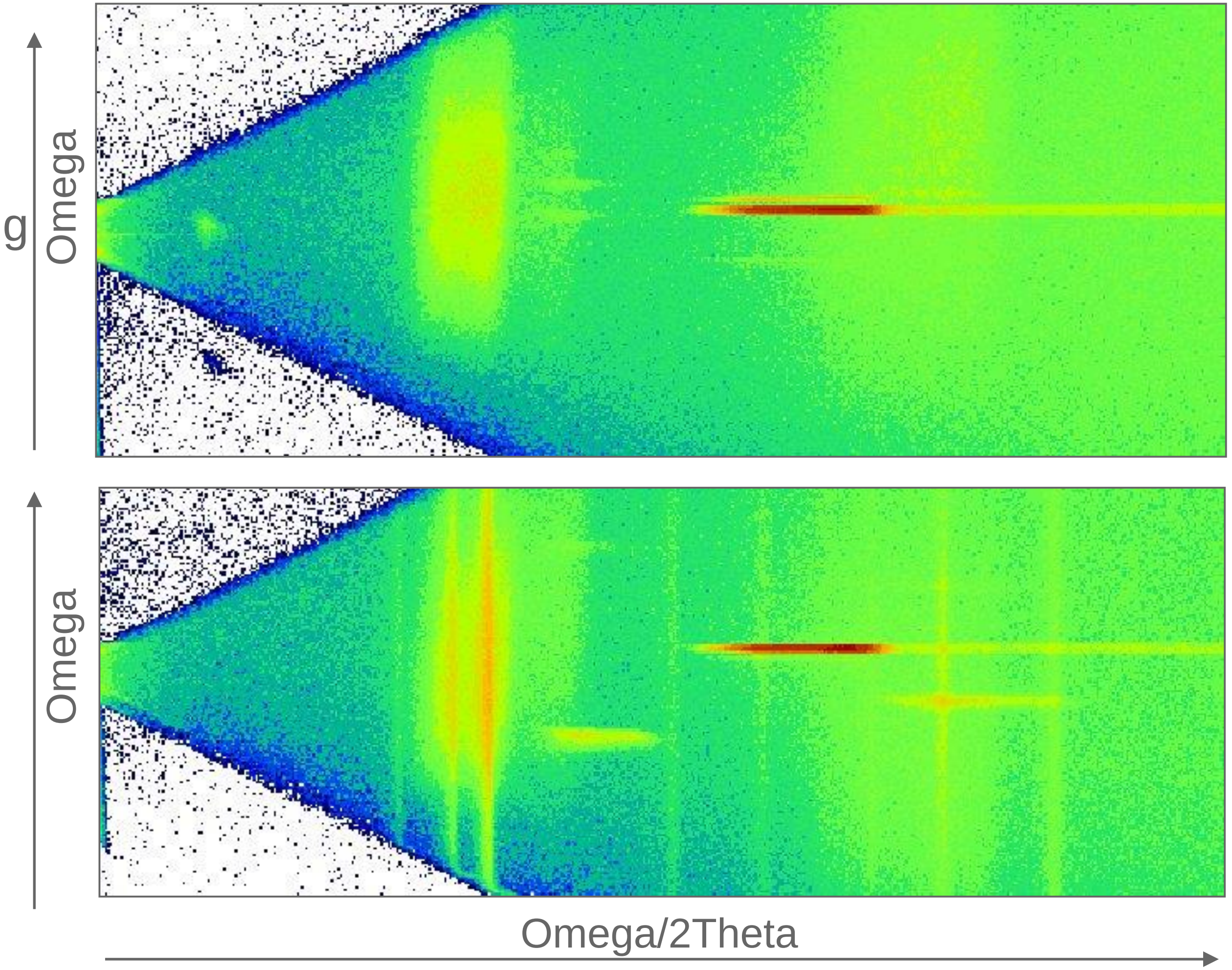

Before annealing

After annealing

2Theta/Omega x Chi Maps

Chi

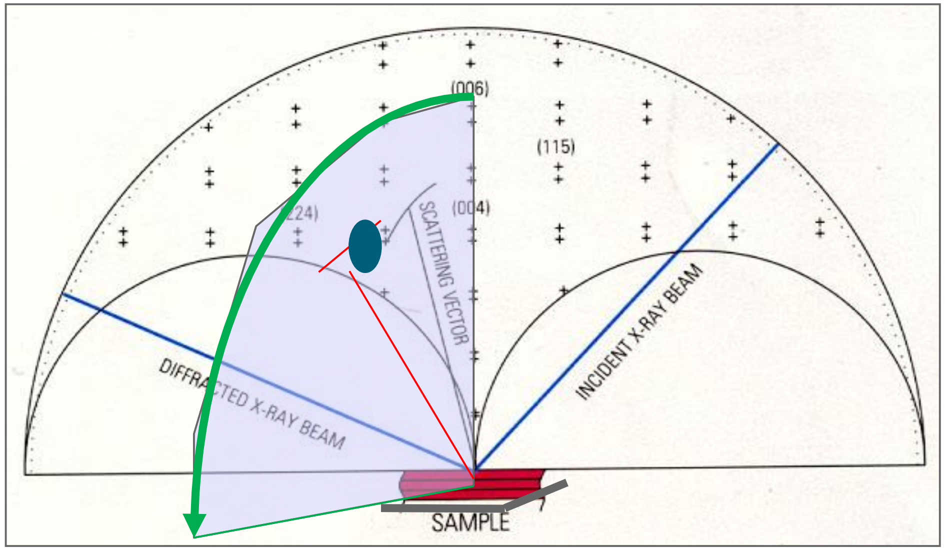

90°

Er2O3 and GaN Peaks

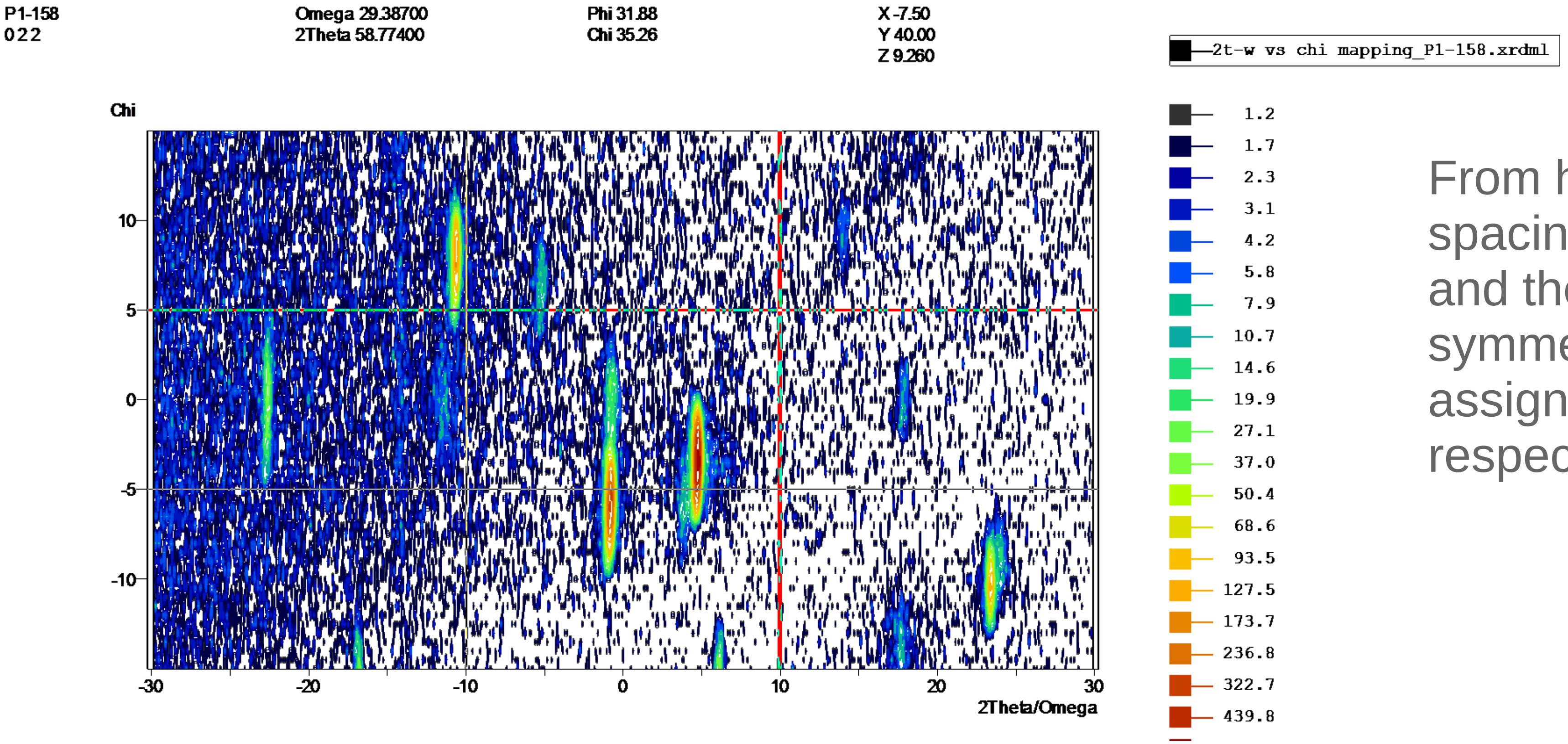

From here, knowing the d-spacing of the reflection and their inclination to the symmetric plane allows to assign peaks of the respective phases.

Literature

1. Fewster P.F. *X-Ray Scattering from Semiconductors* 2nd Edition, Imperial College Press, (2003)
2. Als-Nielsen J. & McMorrow D. *Elements of Modern X-Ray Physics*, Wiley & Sons Ltd, (2001)
3. Batterman B.W. & Cole H. *Rev. of Mod. Phys.* 36(3), 681-717, (1964)